

ATOMIC FORCE MICROSCOPY

AND

ITS APPLICATIONS

THESIS

**Presented to the Graduate Council of
Southwest Texas State University
In Partial Fulfillment of
The Requirements**

For the Degree

Master of SCIENCE

By

Yuji Yamaguchi, B.S.

**San Marcos, Texas
December, 2000**

COPYRIGHT

by

Yuji Yamaguchi

2000

ACKNOWLEDGEMENTS

I like to thank Dr. Heather C. Galloway for her help, support, and knowledge throughout my thesis projects as a thesis advisor. I also like to thank Dr. Victor E. Michalk and Dr. Wilhelmus J. Geerts for being on my thesis committee. I want to extend my thanks to the whole Department of Physics for letting me be comfortable when I came here for the first time in 1996.

I want to thank the following people for helping and encouraging me through my college career at Southwest Texas State University: Kevin Wiederhold, Mike Matheaus, Anival Ayala, Eric Wittry, Paul Person, Nelson White, Charlie Watts, Kelly Fishbeck, and many more. I like to thank to my friends that I made while I lived in Houston for understanding the reasons why I left Houston in 1996 and for being great friends still today. I want to thank my friends in Japan for being great friends throughout the years. I also like to thank my Japanese friends here in San Marcos for letting me relax on the weekends when I needed. I am very thankful to Mr. Jim Edwards and Mrs. Shella Baccus for encouraging me to come back to San Marcos to start over again in 1996.

I like to thank my best friend of my life, Naoki Hosoda for being such a great person throughout my life even though we live in the different countries. Finally, but most importantly, I would like to thank my family, especially my mother, my grandparents, and my brother for supporting, encouraging, and understanding me even at my lowest point of my life so far. Without them, I would not be here. I would like to dedicate this thesis to the people who encouraged me throughout my life.

December 13, 2000

TABLE OF CONTENTS

ACKNOWLEDGEMENTS.....	i
LIST OF TABLES.....	iv
LIST OF FIGURES.....	v-viii

CHAPTER

1	INTRODUCTION.....	1
1.1	Scanning Probe Microscopy.....	1
2	ATOMIC FORCE MICROSCOPY (AFM).....	5
2.1	THEORY OF ATOMIC FORCE MICROSCOPY (AFM).....	5
2.1.1	Components of AFM.....	5
2.1.2	Forces Acting of AFM.....	12
2.2	SCANNER NONLINEARITIES.....	14
2.2.1	Intrinsic Nonlinearity.....	14
2.2.2	Hysteresis.....	15
2.2.3	Creep.....	16
2.2.4	Aging.....	16
2.2.5	Cross Coupling.....	16
2.3	NOISE IN AFM.....	17
2.3.1	Sources of Noise.....	17
2.3.2	Noise Protection.....	19
2.4	SCANNING MODES.....	20
2.4.1	Contact Mode.....	20
2.4.2	Non-Contact Mode.....	21
2.4.3	Intermittent-Contact Mode.....	24
3	OTHER SPM TECHNIQUES USING AFM.....	25
3.1	OTHER SPM TECHNIQUES USING AFM.....	25
3.1.1	Lateral Force Microscopy.....	25
3.1.2	Magnetic Force Microscopy.....	27
3.1.3	Electrostatic Force Microscopy.....	29
3.1.4	Force Modulation Microscopy.....	29
3.1.5	Phase Detection Microscopy.....	30
4	SCANNING CAPACITANCE MICROSCOPY (SCM).....	31
4.1	MOTIVATION FOR SCANNING CAPACITANCE MICROSCOPY.....	31
4.2	THEORY OF SCANNING CAPACITANCE MICROSCOPY (SCM).....	33
4.3	DATA.....	36
4.3.1	Capacitance as a Function of Voltage.....	37
4.3.2	Capacitance as a Function of Set Point.....	39

4.3.3	Capacitance as a Function of Frequency.....	40
4.3.4	Capacitance as a Function of Position on the Wafer.....	42
4.4	NON-CONTACT SCM.....	43
4.5	RCA VIDEODISK TECHNIQUE.....	44
5.	LIQUID CELL.....	47
5.1	THEORY OF MICROCELL.....	47
5.1.1	Modifications.....	48
5.1.2	Operation of Microcell.....	51
5.1.3	Window Replacement.....	52
5.2	CHEMICAL MECHANICAL POLISHING (CMP).....	53
5.3	CMP SIMULATION AT THE ATOMIC SCALE USING AFM.....	54
5.4	EXPERIMENTS.....	56
5.4.1	Samples, Chemicals, and Abrasive Particles.....	56
5.4.2	Copper with HNO ₃ (0.063%) without Benzotriazole (BTA) and a Silica Tip.....	57
5.4.3	Copper with HNO ₃ (0.063%) with BTA and a Silica Tip.....	59
6.	VIDEO CAMERA FOR SPOTTING LASER ON CANTILEVER.....	63
6.1	SET UP.....	63
6.1.1	Stand.....	64
6.1.2	Microscope.....	64
6.1.3	Video Camera and Monitor.....	64
6.2	RESOLUTION.....	64
7.	CONCLUSIONS.....	66
7.1	SCANNING CAPACITANCE MICROSCOPY.....	66
7.2	LIQUID CELL.....	67
7.3	FUTURE WORKS.....	67
	BIBLIOGRAPHY.....	69
	VITA.....	71

LIST OF TABLES

	Page
Table 2.1 Dimensions of cantilever on Microlever chip.....	8-9
Table 2.2 Dimensions of cantilevers on contact Ultralever chip.....	9
Table 2.3 Dimensions of cantilevers on non-contact Ultralever chip.....	9
Table 5.1 Combinations of material, chemical, and abrasive particles used in CMP....	56

LIST OF FIGURES

	Page
Figure 1.1 Interaction between tip and sample in STM.....	2
Figure 1.2 Constant-height mode and constant current mode.....	2
Figure 2.1 AFM system in Dr. Galloway's lab.....	5
Figure 2.2 a) Components of AFM head, and b) inside of AFM showing three legs to move the head.....	6
Figure 2.3 The schematic of contact AFM showing the laser beam is reflected off the top of the cantilever and to the photodiode detector.....	6
Figure 2.4 Two kinds of cantilevers: Microlever on the left and Ultralever on the right..	8
Figure 2.5 The cartridges for contact mode and non-contact mode. The difference between these cartridges is that the cartridge for non-contact mode has piezoelectric material to vibrate the cantilever holder.....	10
Figure 2.6 a) The piezoelectric material used as a scanner in AFM is a tube, b) when the same sign of voltage is applied to the same sign of piezoelectric material orientation, c) when voltage is not applied, and d) the opposite sign of voltage is applied.....	11
Figure 2.7 Forces acting between the tip and the sample are different depending on the separation between them.....	12
Figure 2.8 Intrinsic nonlinearity of the scanner.....	15
Figure 2.9 Effects of hysteresis, creep, and cross coupling.....	17
Figure 2.10 Forces vs. separation between the tip and the sample curve is plotted.....	20
Figure 2.11 The schematic that describes how non-contact mode AFM works. The difference between the contact and non-contact AFM is that the non-contact mode cartridge has a piezoelectric material to vibrate the cantilever holder.....	22
Figure 2.12 The difference between how the images would look with the contact mode and non-contact mode when the sample with a droplet of water is scanned.....	24
Figure 3.1 The difference in the photodiode detectors for AFM and LFM.....	25

	Page
Figure 3.2 Two kinds of LFM deflection: changes in sample feature on the left and changes in friction of the surface on the right.....	26
Figure 3.3 Contact AFM images and LFM images of tungsten film on the tip and copper on the bottom.....	27
Figure 3.4 The schematic that shows how MFM works. The magnetized tip moves vertically corresponding to the magnetic domains of the sample.....	28
Figure 3.5 MFM images of a computer hard drive taken by B. White, E. Wittry, and H. Galloway at SWT.....	29
Figure 3.6 There is difference in the phase lag depending on the mechanical characteristics of the sample.....	30
Figure 4.1 Modification on AFM to take SCM images.....	33
Figure 4.2 The difference in the plots where the amplitude of the signal versus frequency. The plot on the left is $2f$ and $1f$ on the right.....	35
Figure 4.3 Voltage dependence on Moto 3 with both sensitivities.....	37
Figure 4.4 Voltage dependence with 100mV sensitivity on the top, and voltage dependence analysis of capacitance signal.....	38
Figure 4.5 Set point analysis of Moto 3.....	39
Figure 4.6 Set point analysis ($0.5\mu\text{m}$).....	40
Figure 4.7 Frequency analysis of Moto 3-A.....	41
Figure 4.8 SCM images of Moto 3 at different frequencies (from left 44.35kHz, 45.35kHz, and 46.35kHz).....	41
Figure 4.9 How the wafer was cut into pieces A, B, C, and D.....	42
Figure 4.10 Plot of average heights at each section.....	42
Figure 4.11 Topography and non-contact SCM images of Moto 3.....	43
Figure 4.12 Perspective and cutaway views of stylus and coated disk.....	45
Figure 4.13 How SCM with a transmission-line pickup circuit is set up.....	45

	Page
Figure 5.1 Top and side views of a microcell.....	47
Figure 5.2 The diagram that shows how liquid cell works, and it shows that the laser beam must pass through a glass window and liquid before hitting the top of the cantilever. The laser beam then must pass through the liquid and a glass window again to the photodiode detector.....	48
Figure 5.3 The liquid cell technique using the regular cantilever holder and a tub that is made out of Teflon. The sample is set inside of the tub before the liquid is inserted into the tub.....	49
Figure 5.4 The liquid cell system using both the Teflon tub and microcell. This system makes the top of the liquid flat so that spotting the laser beam is easier.....	49
Figure 5.5 The liquid cell with a pump is designed to flow the liquid to keep the temperature of the liquid constant. Another reason we designed this system is to vary the pH of the solution to see the variation in the features on the sample....	50
Figure 5.6 The liquid cell system using only few drops of the solution.....	51
Figure 5.7 a UV curing glue is used to replace the window on the microcell. The microcell is set at the point where a UV light is converged, the focal point of the convex lens.....	52
Figure 5.8 The figures on the left show how the unpolished sample differs from the polished sample. The figure on the right shows how CMP process works. The slurry, which consists of the chemical solution, corrosion inhibitor, and abrasive particles, is poured onto the surface of a polishing pad. Both the wafer and polishing pad rotate in the same direction with pressure applied to them.....	54
Figure 5.9 The figure on the top shows how CMP with a polisher works. The figure on the bottom shows how we simulate the CMP process with AFM. Everything is pretty much the same except the tip of the cantilever is used as the abrasive particles in the CMP process with a polisher.....	55
Figure 5.10 These diagram and picture show how bubbles inside of the liquid cell affects the path of the laser beam.....	57
Figure 5.11 The liquid cell images of copper with nitric acid (HNO ₃) as the chemical. As shown in the images, the features on the sample surely changed. Each image took about two minutes to be imaged.....	58

- Figure 5.12 The images which were taken after $1\mu\text{m}\times 1\mu\text{m}$ images. Ones on the top are $4\mu\text{m}\times 4\mu\text{m}$ images and ones on the bottom are $3\mu\text{m}\times 3\mu\text{m}$ images. In both sizes, almost perfect square of $1\mu\text{m}\times 1\mu\text{m}$ can be seen where we took $1\mu\text{m}\times 1\mu\text{m}$ images earlier. Two images on right are images that were flattened by the software correction..... 59
- Figure 5.13 These diagrams show how the solution with corrosion inhibitor like BTA would create a monolayer on top of the sample. When the solution with BTA makes contact with the sample, the monolayer of BTA molecules is laid. Only the area the tip on the cantilever makes contact is where CMP process occur... 60
- Figure 5.14 The liquid cell images of copper with nitric acid (HNO_3) with BTA. Once again the features on the sample changed. Also, the RMS roughness of images decreased as more images are taken. Each image took about two minutes..... 61
- Figure 5.15 The image on the right is taken at $1\mu\text{m}\times 1\mu\text{m}$ in the image. The roughness is smaller than the images taken with the solution without BTA in it. The image on the right is $1\mu\text{m}\times 1\mu\text{m}$ image. Within the image, we are able to see both $1\mu\text{m}\times 1\mu\text{m}$ and $3\mu\text{m}\times 3\mu\text{m}$ squares..... 61
- Figure 6.1 Video camera system designed to make focusing the laser beam on the top of the cantilever easier..... 63
- Figure 6.2 To see the resolution of the video camera system, we looked at two objects. One on the left is the Microlever, which has the smallest feature of $18\mu\text{m}$. We then looked at a $9.9\mu\text{m}$ grating, which we were able to see..... 65
- Figure 7.1 The force vs. distance curve..... 68

CHAPTER 1

INTRODUCTION

1.1 Scanning Probe Microscopy

Scanning Probe Microscopy (SPM) is the technique that uses a small tip to scan over a sample to map its topography and to study its surface properties from the atomic to the microscopic level. The invention of Scanning Tunneling Microscopy (STM) by Gerd Binnig and Heinrich Rohrer at IBM Zurich in 1981 sparked the SPM industry ¹. Binnig and Rohrer were awarded the Nobel prize in physics in 1986 for STM invention.

In the STM, a potential difference is applied between the tip and sample. When the tip and sample are a small distance away from each other ($\sim 10 \text{ \AA}$) ², the electrons are able to tunnel through the dielectric barrier (vacuum, air, or liquid) due to the quantum tunneling. The tunneling current varies exponentially with the separation distance between the tip and sample.

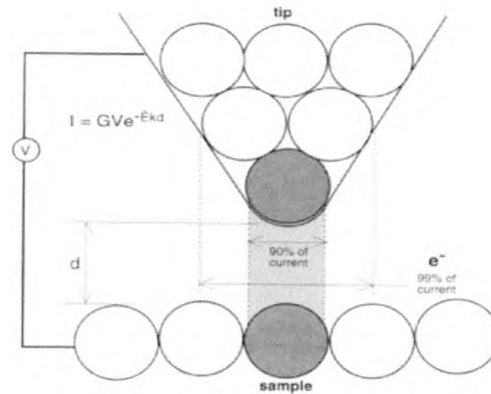


Figure 1.1 Interaction between tip and sample in STM ³.

Because tunneling current varies exponentially with the distance between electrodes, when the distance changes by 10% the tunneling current varies by one order of magnitude³. A computer records the tunneling current and maps the sample's topography. This mode is called the constant-height mode because the tip does not move vertically. The other mode that STM can use to map the topography of a sample is the constant-current mode in which the feedback loop is used to control the motion of a tip to keep the tunneling current constant. Because the STM does not have to move the scanner vertically in the constant-height mode, this mode is faster than the constant-current mode. The disadvantage of constant-height is that this mode only works for very smooth surfaces. The figures below show the difference in these two modes in STM.

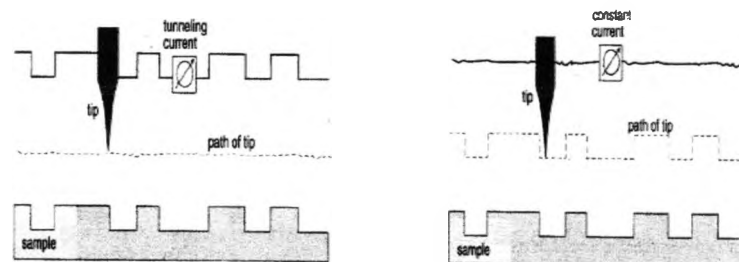


Figure 1.2 Constant-height mode and constant current mode ³.

Atomic Force Microscopy (AFM) is another type of SPM. One of AFM's advantages over STM is that, because a potential difference is not needed to be applied to take topographic images, the sample can be an insulator.

In my thesis, I will discuss the Atomic Force Microscopy (AFM) and the various techniques using AFM. Several examples will demonstrate the various capabilities of different modes. The thesis includes a discussion of how AFM works, its components, and forces acting on the AFM. We then discuss the scanner nonlinearities in AFM. This is important to understand how software and hardware corrections work to image the sample closely as to what actual surfaces look like. Because AFM images the surface in a very small area, it is crucial not to have any kind of noise around the AFM. We use an instrument that can plot the intensity versus frequency to see the sources of noise and how to protect the AFM from noise. There are three scanning modes in AFM. They are contact mode, non-contact mode and intermittent (tapping) mode.

Different Scanning Probe Microscopy (SPM) techniques are possible with our equipment. Lateral Force Microscopy (LFM) is used to see the friction force between the tip and the sample. Magnetic Force Microscopy (MFM) images the magnetic characteristics of the sample using a magnetized tip. Electrostatic Force Microscopy (EFM) uses the same concept as MFM except EFM uses an electronically charged tip to image the electric characteristics of the sample. Phase Detection Microscopy (PDM) is used to image the variation in properties like elasticity and adhesion. Force Modulation Microscopy (FMM) is the technique used to map the mechanical properties of the sample. We discuss how these techniques work and show examples of some techniques.

Scanning Capacitance Microscopy (SCM) is a technique that can image dielectric properties of the sample. We explain how SCM works theoretically, and show how to modify an AFM to take SCM images. We then analyze a sample grown by Motorola. Using the detailed characteristics of the sample, we performed different experiments to see if our data are consistent with their data.

Microcell (liquid cell) is a component added to AFM to take topographic images of the sample inside of a liquid. We discuss components of the microcell and how it works. Because the microcell is built for liquids with high surface tension, we made modifications for liquids with lower surface tension. These modifications are shown. The purpose of using the microcell to take AFM images inside of different solutions is to understand Chemical Mechanical Polishing (CMP) used in the integrated circuit manufacturing process at the atomic scale.

Finally, we will discuss the video camera system used to focus the laser on top of the cantilever. We show the components of this system and how to operate the system. We also discuss the resolution of the system.

CHAPTER 2

ATOMIC FORCE MICROSCOPY (AFM)

2.1 Theory of Atomic Force Microscopy (AFM)

2.1.1 Components of AFM

The figures below show components of the Atomic Force Microscope (AFM) system in Dr. Heather Galloway's lab.



Figure 2.1 AFM system in Dr. Galloway's lab

The laser and photodiode detector are located in the head of AFM, which moves vertically with the help of three fine screwed legs. The figures below show the head of AFM and two of the three screws mentioned above.

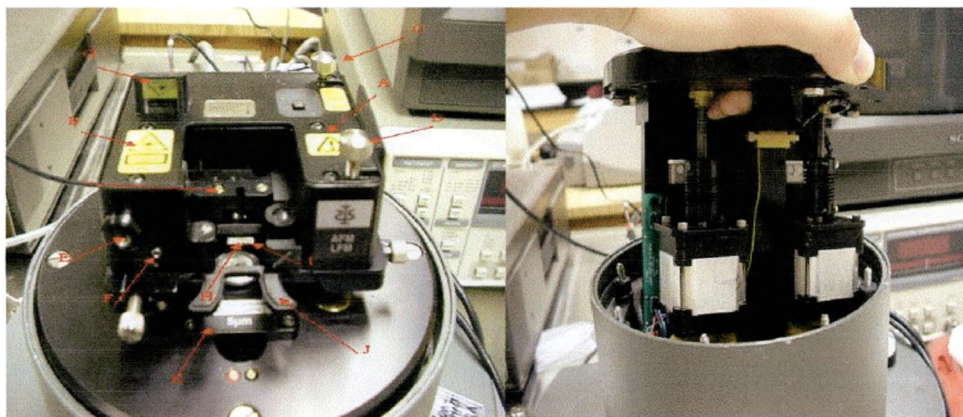


Figure 2.2 a) Components of AFM head, and b) inside of AFM showing three legs to move the head
 The laser is mounted on the right side of the head (A in Fig. 2.2), and the detector is mounted on the left side of the head (B in Fig. 2.2). The circular detector is separated in two sections, labeled A and B in the figure below, for regular AFM mode. The first thing we must do before taking any kind of images is to focus the laser to reflect off the top of a cantilever (a tip is attached underneath it) and let the reflected laser beam hit the photodiode detector as can be seen below:

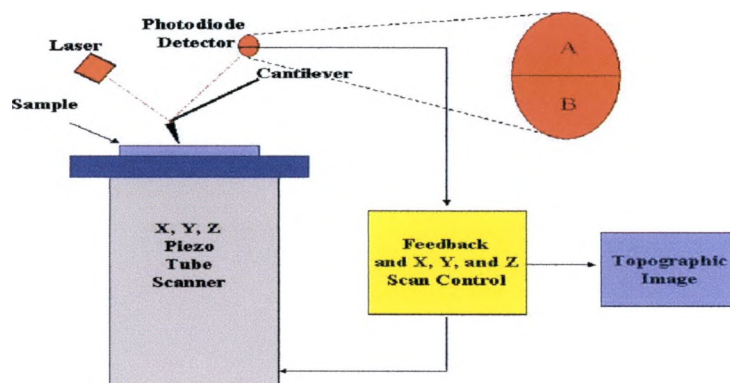


Figure 2.3 The schematic of contact AFM showing the laser beam is reflected off the top of the cantilever and to the photodiode detector.

The position of the laser beam is controlled by two screws (C and D in Fig. 2.2). It takes some time to get used to setting the laser beam on the cantilever because they move

diagonally. The reflected laser light on the photodiode detector creates some current, which is then converted to a voltage signal. The more light hits the detector, the more current is created. Voltages on A and B are reported by digital voltmeters in the software program we use to operate the AFM. We need two digital voltmeters for basic AFM imaging. One of them is called A+B. This is the sum of the voltages measured by segments of the photodiode A and B. For accurate imaging, we want this voltage to be as large as it can be (about 1.5V to 2V). The other digital voltmeter is called A-B, and it measures the difference of A and B voltages. To set the laser at the center of the photodiode detector, we want this voltage to be as low as possible ($100\text{mV} < x < 100\text{mV}$). The A-B signal has 10X more gain than the A+B signal. This number can be negative because it just means that the laser is spotted more on the B-side. Two screws, E and F in Fig. 2.2, are used to move the photodiode detector. The screw E moves the detector vertically, and it is used mostly when we are using Lateral Force Microscopy (LFM), which will be discussed in the later chapter. The screw F controls the horizontal motion of the detector. This screw also controls the A-B signal. When the A-B signal needs to be more negative, the screw is turned counterclockwise. It is turned clockwise for making it more positive. Another way to check whether the laser is spotted on the detector is to see the laser intensity and position indicator located at G in Figure 2.2. The indicator has a green LED at the center of it, and a green LED is surrounded by either two or four red LEDs depending on which head is used. A green LED indicates that the laser beam is on the detector. But when the magnitude of A-B signal is larger than 200mV, the red LEDs turn on. When there is a green LED lit and not a red one, the laser is set properly on the detector.

After making sure that the laser is spotted on the detector properly, we may press the “Approach” button to lower the head automatically to the sample. As the cantilever scans through a sample, the cantilever moves vertically corresponding to the surface of a sample. Depending on the bending of the cantilever, the reflected laser will spot a different position on the detector. The variation of the A-B signal is recorded. A feedback mechanism controls the scanner. A computer then maps the topography. This is the basic concept of how an AFM works.

In Dr. Heather Galloway’s lab, we have two different kinds of chips with cantilevers, the Microlever and the Ultralever. The figure below shows both kinds of chips.

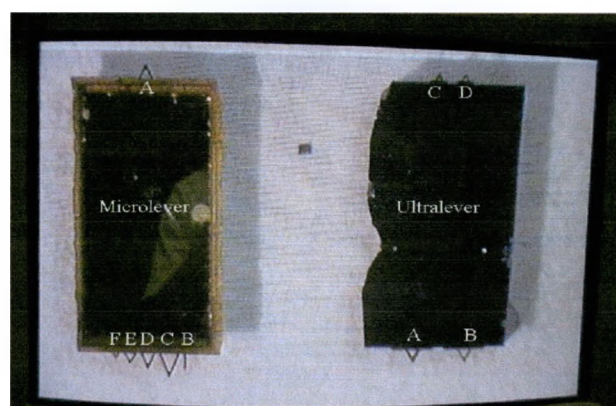


Figure 2.4 Two kinds of cantilevers: Microlever on the left and Ultralever on the right

One type is called Microlevers, and they are used for general purpose imaging. They are made out of silicon nitride, and the top of them is coated with gold for high reflectivity. They consist of one cantilever on one side and five cantilevers on the other side. Each cantilever has the same thickness, but a different length, width, force constant and resonant frequency. A table below shows all dimensions and other parameters.

Table 2.1 Dimensions of cantilevers on Microlever chip ³

Cantilever Type	A	B	C	D	E	F
Length (μm)	180	200	320	220	140	85
Width (μm)	18	20	22	22	18	18
Thickness (μm)	0.6	0.6	0.6	0.6	0.6	0.6

Force Constant (N/m)	0.05	0.02	0.01	0.03	0.1	0.5
Resonant Frequency (kHz)	22	15	7	15	38	120

The second type of chips is called Ultralevers. They have two silicon cantilevers with silicon conical tips on each side of the chip. These cantilevers are used for maximum resolution. Ultralevers are doped with boron for lower resistivity of $0.001 \Omega \cdot \text{cm}^3$. Like Microlevers, the top of Ultralevers are coated with gold for high reflectivity. There are two kinds of Ultralevers. One is used for contact mode, and the other one is for intermittent/non-contact mode. These AFM modes will be discussed in the later section. Typical dimensions and parameters for the contact Ultralever are listed below:

Table 2.2 Dimensions of cantilevers on contact Ultralever chip³

Cantilever Type	A	B	C	D
Length (μm)	180	180	85	85
Width (μm)	25	38	18	28
Thickness (μm)	1	1	1	1
Force Constant (N/m)	0.26	0.4	1.6	2.1
Resonant Frequency (kHz)	40	45	140	160

The non-contact Ultralevers have the same length and width as the contact Ultralevers do, but have different thickness, force constant, and resonant frequency. Both force constant and resonant frequency for non-contact Ultralever are much higher than those of contact Ultralever. The parameters for non-contact Ultralever are listed below:

Table 2.3 Dimensions of cantilevers on non-contact Ultralever chip³

Cantilever Type	A	B	C	D
Thickness (μm)	2	2	2	2
Force Constant (N/m)	2.1	3.2	13	17
Resonant Frequency (kHz)	80	90	280	320

Proper cantilevers are chosen for a certain experiment. For example, if we need to apply voltage to the cantilever it is better to use Ultralevers because it has lower resistivity.

Also, if a certain resonant frequency of a cantilever is needed, we can check the tables above.

The cantilever (H in Fig.2-2) is mounted on a cantilever holder (I in Fig.2-2). There are two kinds of cantilever holders. One of them is used for regular AFM modes. The other one is used when a voltage needs to be applied to the cantilever. This cantilever holder has an insulator between the cantilever holder and cantilever when it is mounted so that the voltage is only applied to the cantilever. The pictures of both cartridges follow.

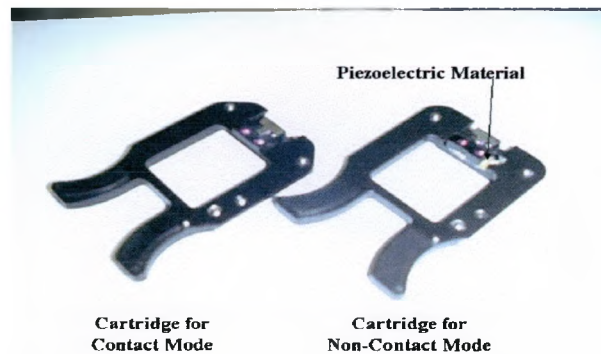


Figure 2.5 The cartridges for contact mode and non-contact mode. The difference between these cartridges is that the cartridge for non-contact mode has piezoelectric material to vibrate the cantilever holder.

The cantilever holder is then mounted on one of two cartridges depending on what mode is needed for the experiment. The cartridge is mounted on AFM (J in Fig.2-2). The first kind is used for contact mode, and the other one is used for both intermittent and non-contact modes. There are two differences in these cartridges. One of them is that the cartridge for non-contact mode contains the piezoelectric material to vibrate the cantilever holder at a specified frequency. The second difference is that there is a metal

connection on the non-contact mode cartridge so that an electric potential can be applied between the tip and the sample.

The scanner is mounted on the AFM (K in Fig.2-2). The scanner uses piezoelectric material to move the sample in different directions. Piezoelectric is a polycrystalline ceramic material, which shrinks, extends, or bends depending on how voltage is applied to it. The piezoelectric material is polarized. The piezoelectric material used in the scanner is a tube, which is separated into four sections. The diagrams below show how piezoelectric works.

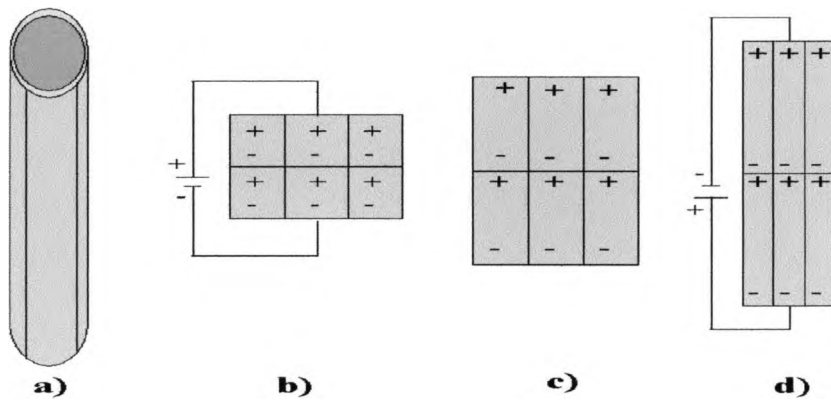


Figure 2.6 a) The piezoelectric material used as a scanner in AFM is a tube, b) when the same sign of voltage is applied to the same sign of piezoelectric material orientation, c) when voltage is not applied, and d) the opposite sign of voltage is applied.

Although the shape of piezoelectric material changes when voltage is applied, the volume of it does not change. By applying the same sign and magnitude of voltage to all four sides of the piezoelectric tube with the interior kept at ground, the tube will either extend or shrink depending on whether the voltage is positive or negative. When different voltage is applied to one section of the piezoelectric and the same voltage on others, a piezoelectric will bend toward the section with different voltage. The displacement of the piezoelectric material depends on length, thickness, and voltage applied. In our lab, we

have a $5\mu\text{m}$ scanner and a $100\mu\text{m}$ scanner. With the $5\mu\text{m}$ scanner, we are able to take images with a maximum size of $5\mu\text{m} \times 5\mu\text{m}$. Similarly, with the $100\mu\text{m}$ scanner the limit of the scanning range is $100\mu\text{m} \times 100\mu\text{m}$. The main difference between these scanners is the heights of the piezoelectric material inside of the scanner. The advantage of the $5\mu\text{m}$ scanner over the $100\mu\text{m}$ scanner is that we are able to get higher resolution in a small scanning range due to its capability of a more precise motion of the piezoelectric material. The $100\mu\text{m}$ scanner has the advantage of software linearity correction, which cannot be operated with the $5\mu\text{m}$ scanner.

2.1.2 Forces Acting on AFM

Forces in AFM are very important. There are a few different forces acting between the tip and sample that cause the cantilever to bend or deflect. Here is a graph which shows which forces act at a certain separation between the tip and the sample.

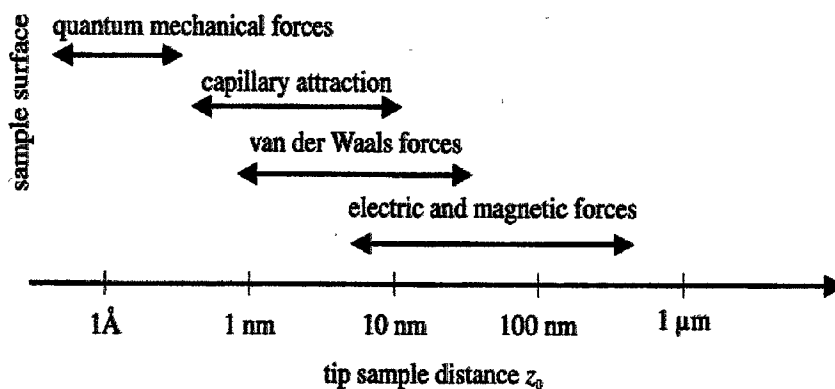


Figure 2.7 Forces acting between the tip and the sample are different depending on the separation between them ⁴.

The most common force acting between the tip and sample is called van der Waals force. It is a distance dependent attractive force that occurs when the tip induces weak dipoles in the sample or vice versa. The van der Waals force for the object above the sample varies as the inverse fifth or sixth power of the separation. As the separation increases,

the inverse power of the separation decreases. As can be seen in the Fig. 2.7, electric and magnetic forces act when the separation is large. The electric and magnetic forces varies as the inverse square of the separation. When the atoms in the tip and the atoms in a sample act as a weak electric dipole, they feel an electrostatic attraction between them. When the tip is approaching to the sample, the tip and the atoms in the sample start to feel the attractive force. The attractive van der Waals force dominates until the tip and the atoms in the sample are a few angstroms away from each other. At this distance, the repulsive force dominates the attractive force. The repulsive force becomes stronger as the distance between the tip and the atoms in the sample gets smaller due to the electron clouds of each side overlapping. Unless the force exerted by the cantilever is bigger than the bond strength of the sample atoms, the atoms are not able to get closer than this point. On the other hand, if the force per atom exerted by the cantilever were larger than the bond strength of the sample atoms, the atomic bonds in the sample would be broken.

Another common force acting on to tip of the AFM system is called the capillary force. The capillary force is the force, which occurs due to the liquid layer on the sample. The humidity of air produces a thin layer of liquid on the sample. The magnitude of this force depends on the distance between the tip and sample. As long as the tip is in contact with the sample, this force should be approximately constant. Because this force is due to the liquid layer on the sample, there are few ways to avoid this force. One of the ways is to operate AFM in vacuum. The vacuum must be less than 10^{-3} torr³. Another way to eliminate the capillary force is to submerge the AFM system (the tip and sample) in a liquid cell. This technique will be discussed in chapter 5.

The force exerted by the cantilever is like the force of a compressed spring. The magnitude and sign (repulsive or attractive) of the cantilever force depend upon the deflection of the cantilever and upon its spring constant, respectively. The total force that the tip exerts on the sample is the sum of the capillary force plus cantilever forces.

2.2 Scanner Nonlinearities

Ideally, what we want in characteristics of a piezoelectric material is that, when voltage is applied to it, the strain (a term for the ratio of the change in length of piezoelectric material to the original length, $\Delta y/y$) varies linearly. An equation describing this ideal relationship follows:

$$S = d \cdot E \quad \text{Equation 2.1}$$

Where S is the strain ($\text{\AA}/\text{m}$), E is the electric field applied (V/m), and d is the strain coefficient ($\text{\AA}/\text{V}$). Depending on what kind of piezoelectric material is used, the strain coefficient is determined. As stated above, the condition described above is the ideal case. The actual experiments do not agree with the theory above, and there are many nonlinearities in a scanner.

2.2.1 Intrinsic Nonlinearity

The first nonlinearity is called the intrinsic nonlinearity. When the voltage applied to the piezoelectric material and the extension of it used by this voltage are plotted, the graph should be a straight line in the ideal case. But the graph in the actual experiment is non-linear.

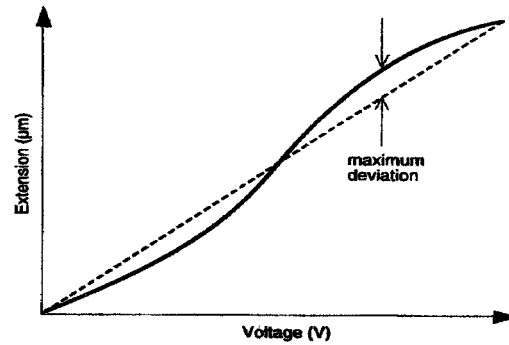


Figure 2.8 Intrinsic nonlinearity of the scanner ³

The degree of the intrinsic nonlinearity is described by the percentage, which is calculated by dividing the maximum deviation Δy from the ideal straight line by the ideal linear extension y at that voltage. Because the piezoelectric material does not extend or shrink linearly, the image for a well-spaced sample will have non-uniform spacing. This nonlinearity applies to all three dimensions.

2.2.2 Hysteresis

The hysteresis behavior of the piezoelectric material is another type of nonlinearity. Suppose we apply voltage to the piezoelectric material starting at zero, increase until some voltage, and decrease the voltage back to zero. The graph of decreasing voltage does not retrace the graph of increasing voltage. This type of graph is called a hysteresis curve. The degree of hysteresis is described by the ratio of the divergence between the two curves to the maximum extension by a voltage. The AFM is capable of taking images in two directions. Due to the hysteresis of the scanner, one image is shifted slightly from the other one. Shift is also caused by the torsion of the tip. When a scanner scans up and down a step of the same height, more voltage is required to go down the step than going up. So the image taken by AFM will have bigger displacements when a scanner is stepping down, but this is a small effect.

2.2.3 Creep

Creep is the nonlinearity that is caused because the scanner is not able to react to an abrupt change in the features of the sample. So instead of a sharp corner, the AFM image will have a rounded corner. The difference in extension of the scanner from the point where the rounded corner begins to the point where it ends is called the creep.

2.2.4 Aging

The parameter of the strain coefficient, as explained above, varies exponentially with time and use. When the extension of a piezoelectric material and time is plotted, the graph for the scanner used regularly, shows the extension slowly increases exponentially. The graph for a scanner not used regularly, show the extension gradually decreases. As explained above, piezoelectric material is a polycrystalline material, and each crystal in the material has its own dipole moment. When the voltage is applied to the piezoelectric material regularly in the same direction, more and more dipoles start to align in that direction. Because the deflection of the piezoelectric material depends on how many dipoles are aligned in that direction, more use causes larger deflection. When the scanner is not used often, the dipoles in the piezoelectric material crystals begin to lose their alignment. This causes fewer crystals to contribute to the deflection of the scanner.

2.2.5 Cross Coupling

The last type of nonlinearity that we are going to mention is called cross coupling. Because the scanner bends in x and y directions by extending one side of tube and shrinking the other side, the scanner moves in an arc, instead of moving in the plane of a sample. This nonlinearity causes the images to have a bowl-shape without any

correction. But our AFM is capable of subtracting the background curves using software correction called the image processing software.

Most of the time, all of these nonlinearities are present. When the hysteresis, creep, and cross coupling occur in a single step imaging, the image looks like the following:

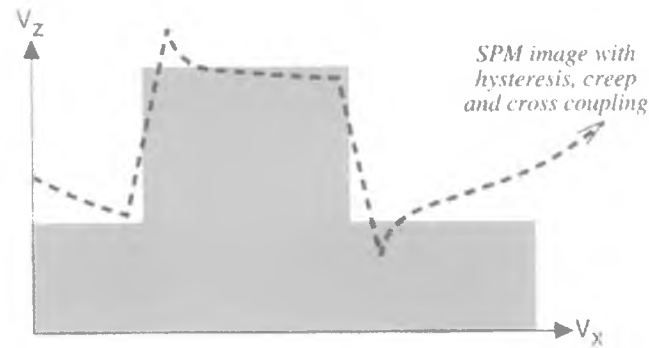


Figure 2.9 Effects of hysteresis, creep, and cross coupling ³

In Fig.2.9, the effect of creep can be seen at the points where corners are rounded. Cross coupling causes the whole image to have arc shape, which can be seen both right and left hand sides of the feature. The left side of the SPM image in Fig.2.9 is higher than the right side due to the effect of hysteresis.

2.3 Noise in AFM

2.3.1 Sources of Noise

In experiments with AFM, noise can affect our results. One of the sources of noise is electrical from the devices around it. The electronic devices around AFM (including computer to operate AFM, video camera, monitor, lock-in amplifier, and other electrical like lights) have power supplied at 60Hz. This frequency is the most common noise, and it is difficult to eliminate it.

Another type of noise we must worry about is physical vibration. Because AFM scans a small area, vibration on AFM can be crucial. It is important not to shake the AFM and a table that supports it. We also must be careful not to slam a door or talk too loudly. On top of these physical problems, the AFM itself has system noise. The AFM noise also includes the resonant frequencies of the building and table. There are two ways to measure the system frequency. One of the ways is to set the scanning range to zero when the tip is approached to the sample. By doing so the tip is stationary, and the tip, sample, or both vibrate at the system frequency. After taking an image with the scanning range of zero, go to the software called Proscan Image Processing in which we are able to analyze the image line by line. When an image is taken at 1Hz, analyzed on an arbitrary line, and it has 60 bumps on the cross-sectional display, the result tells us that the system frequency is 60Hz. If there were too many bumps at low frequencies, increasing the imaging frequency will make the display easier to read.

The second way to measure the system frequency of AFM is to use a RHK Control Electronics Model STM 100. This device is usually used to control an STM. A LV Signal Access Module box is a box that has five BNC connections, and one of them gives A-B signal depending on the internal connections. What we can do is to get A-B signal from this box and put the signal to an auxiliary connection of a RHK box. The software that operates a RHK box can do the fast Fourier transformation. The computer plots the intensity on y-axis and the frequency on x-axis. By looking at the plot, we are able to detect the system frequency of AFM.

The software we use to get noise spectrum is called SPM32. There are few parameters we must control when the plots are taken. To get the parameter box in

SPM32 program, we can either press F1 button or right click on the mouse, Acquire, Setup Acquire, and then Power Spectrum. The first parameter is the data source. This depends on which one of inputs on back of RHK box we use. We usually use AUX. Data range is the highest magnitude of voltage the software can handle. The highest value is +/-10V. This parameter needs to be reduced if the signal is too low. The “points to acquire” is the number of points the software will take as data to plot. This parameter depends on how much resolution we want. A set of 64k points is usually sufficient. The “sampling rate” determines the frequency range, and this depends on which frequency we are interested in. We usually use around 40kHz. To acquire the plot, just click on “noise power spectrum” where it says “OFF” when you open the parameter box.

2.3.2 Noise Protection

To protect from electrical and acoustical noises, the AFM has a lid over the head. This lid creates a Faraday cage. The basic idea of the Faraday cage is to surround the AFM system by a continuous grounded conductor to prevent the entry of electrical signals from outside of the lid. This concept is used in BNC cables, which we use to connect to the system. The lid also shuts out light around the AFM. By doing so, only the reflected light off the cantilever is detected by the photodiode detector. This is important because the room lights have a small flicker at 60Hz.

To protect the AFM from mechanical vibration, the AFM is placed on a pneumatic table, which can be floated by air pressure. Air pressure of ~65-75 psi is needed to lift this table. The top weighs about 700lb, and it took six people to carry it. This table isolates the microscope from the building vibrations. Another protection from mechanical vibration is the construction design of the room that the AFM is located at.

The slab is isolated from other rooms of the building so that the building vibrations can be limited. Also, there are several cushions inside the AFM to isolate the head, scanner, and sample from the pneumatic table.

2.4 Scanning Modes

There are three types of scanning modes in our AFM. They are contact mode, non-contact mode, and intermittent mode. When the force versus distance is plotted for AFM, it would look like the diagram below:

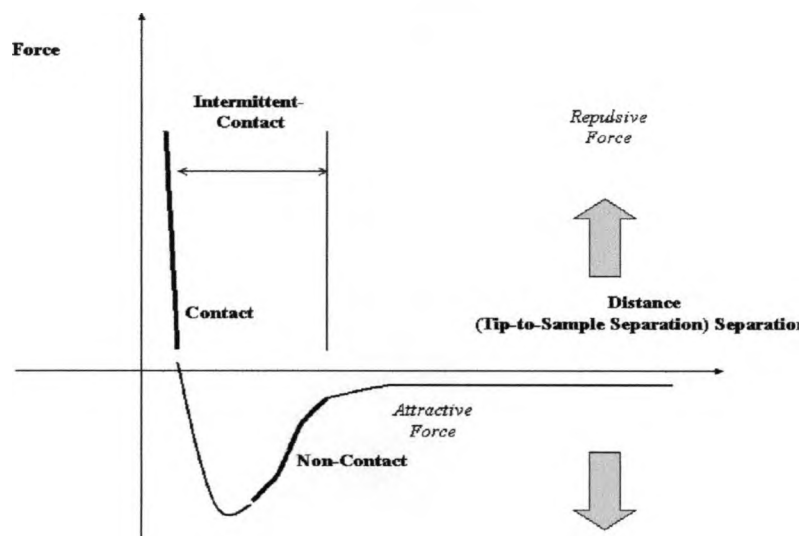


Figure 2.10 Forces vs. separation between the tip and the sample curve is plotted ³.

As can be seen on this diagram, each mode has its own regime. Depending on what kind of sample we use and what surface properties we are interested in measuring, we can decide which mode to use to image. These modes are the subject of this section.

2.4.1 Contact Mode

Contact mode is the mode where the tip on the cantilever physically makes contact with the sample to scan the surface of a sample. The bending of a cantilever due to the contact force is measured with the photodiode detector using the reflected laser off the

top of a cantilever. This mode is usually used for a hard surface sample. When a tip is brought closer and closer to the sample, a tip feels the attractive force. This attractive force increases until the point where the electron clouds of the tip and the sample create the repulsive force. At the point where atoms of the tip and the sample are a few angstroms apart (about the length of a chemical bond), the force between them goes to zero. As the distance attempts to decrease, the repulsive force dominates the attractive force. But the distance cannot get closer than a bond length. In AFM, this is the point where the tip makes contact with the sample.

There are two kinds of mode in contact mode. The most common mode used in AFM is called the constant force mode. In this mode, the feedback loop circuit that operates the scanner applies voltage to the scanner to keep the A-B signal constant, which relates to the deflection of cantilever. By keeping the deflection of cantilever constant, the total force applied to the sample by the tip is also constant.

The second kind is called the constant height mode and is not as common as the constant force mode in AFM. In this mode, the scanner does not move vertically as it does in the constant force mode. As the tip scans the sample, the cantilever moves vertically. This causes the spot of the reflected laser beam to move over the photodiode detector. The computer records the A-B signal for a grid of 256x256 data points to map the topography.

2.4.2 Non-Contact Mode

In non-contact mode, the cantilever vibrates at close to the resonant frequency as measured off the sample. The average separation between the tip and the sample is on the order of tens to hundreds of angstroms. Applying an oscillating voltage to the

piezoelectric material on the non-contact cartridge vibrates the cantilever. The diagram below shows how non-contact mode works:

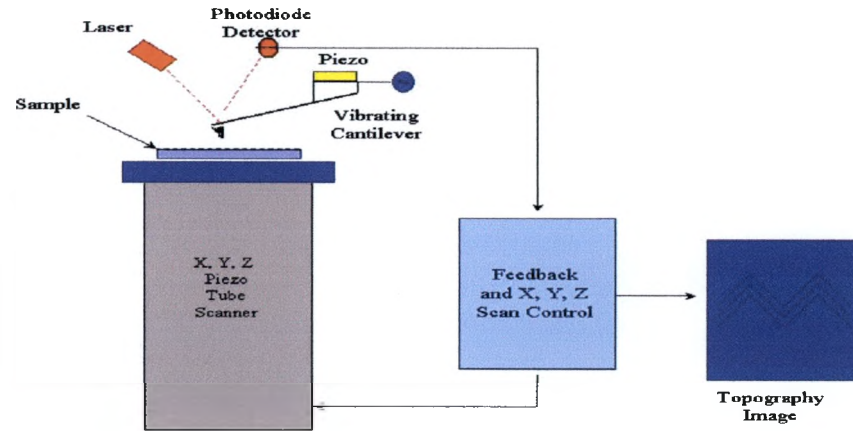


Figure 2.11 The schematic that describes how non-contact mode AFM works. The difference between the contact and non-contact AFM is that the non-contact mode cartridge has a piezoelectric material to vibrate the cantilever holder.

As seen on the force versus distance curve, the non-contact regime is on the attractive force side of the graph. The computer detects the resonant frequency due to change in small attractive force, and the feedback loop applies a voltage to the scanner to keep the resonant frequency constant.

To understand the relation between the resonant frequency of a cantilever and variations in sample topography can be explained as follows. The resonant frequency of a cantilever varies approximately as the square root of its spring constant:

$$\omega = (k_{\text{eff}} / m)^{1/2} \quad \text{Equation 2.2}$$

where ω is the resonant frequency, k_{eff} is the effective spring constant and m is the mass.

The effective resonant frequency is affected by the gradient of the total force between the tip and the sample S :

$$k_{\text{eff}} = [k - (\partial F / \partial x)] \quad \text{Equation 2.3}$$

where k is the spring constant of the cantilever and F is the total force. A term $\partial F / \partial x$ is needed because the force gradient varies as the separation between the tip and the sample changes. The negative sign in this equation is there because we assume that the positive x direction is pointing away from the sample. So the first equation above becomes:

$$\omega = \{ [k - (\partial F / \partial x)] / m \}^{1/2} \quad \text{Equation 2.4}$$

Finally, the force gradient changes with tip-to-sample separation. Thus, changes in the resonant frequency of a cantilever can be used as a measurement of changes in the force gradient, which reflect the topography of a sample.

There are two main reasons that non-contact mode is more difficult to get topographic images than contact mode. One of them is that the total force between the tip and the cantilever is so small that it is hard to detect. The second reason is that for the non-contact mode we must use a stiffer cantilever than for the contact mode because if the cantilever is too soft, the cantilever is pulled towards the sample so hard that it breaks.

The advantage of non-contact mode over contact mode is that it can image a sample with a soft surface without degrading the sample. The disadvantage is that if there is a droplet of water on the sample and non-contact mode is used, the cantilever feels the change in the resonant frequency over the water. Due to this change, the non-contact topography would look different from what contact topography would look like. The diagrams below show the difference in the two modes. This could be used to detect water or other liquids on the sample.

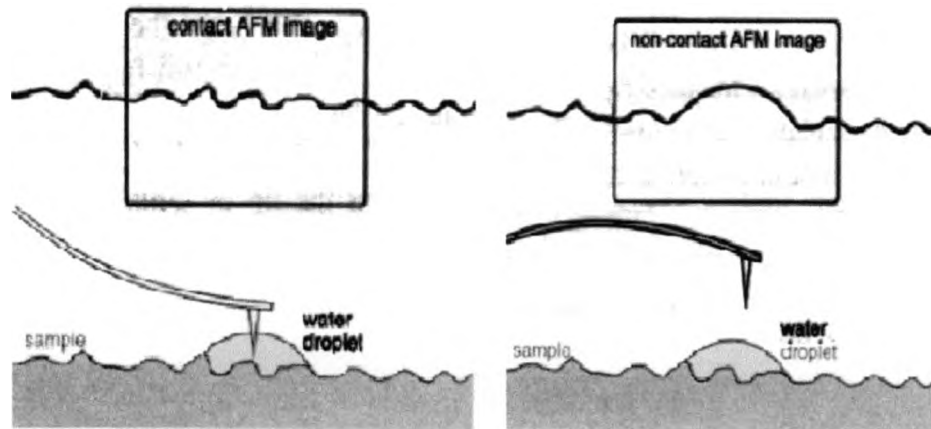


Figure 2.12 The difference between how the images would look with the contact mode and non-contact mode when the sample with a droplet of water is scanned ³.

2.4.3 Intermittent-Contact Mode

In the intermittent-contact mode, the cantilever vibrates, as in non-contact mode, with help of the piezoelectric material mounted on the non-contact cartridge. The difference between these two modes is that in the intermittent-contact mode the tip is brought closer to the sample until the point where the bottom part of cantilever's oscillation actually taps the sample. Because of this mechanism, this mode is also often called the tapping mode. Like the non-contact mode, the amplitude of this oscillation varies as the space between the tip and the sample changes, and the amplitude is recorded to map the topographic images of the sample. The advantage of the intermittent-contact mode over the contact mode is that the sample is less likely to be damaged because the tip only makes contact when it is at the bottom of the oscillation. The advantage of the intermittent-contact mode over the non-contact mode is that the AFM can detect a larger signal because the cantilever is closer to the sample. When the cantilever is closer to the sample the vibration of the cantilever is bigger, and that makes the signals easier to be detected.

CHAPTER 3

OTHER SPM TECHNIQUES USING AFM

3.1 Other SPM Techniques using AFM

AFM can be used to measure many other characteristics of the sample besides its topography with some modifications. In this section, we would like to discuss a few techniques: Lateral Force Microscopy, Magnetic Force Microscopy, Electrostatic Force Microscopy, Phase Detection Microscopy, and Force Modulation Microscopy. In the next chapter, we will discuss scanning capacitance microscopy.

3.1.1 Lateral Force Microscopy

In Lateral Force Microscopy (LFM), we must use a different head called LFM. Unlike the head we explained earlier, the LFM head contains a photodiode detector that is separated into four sections.

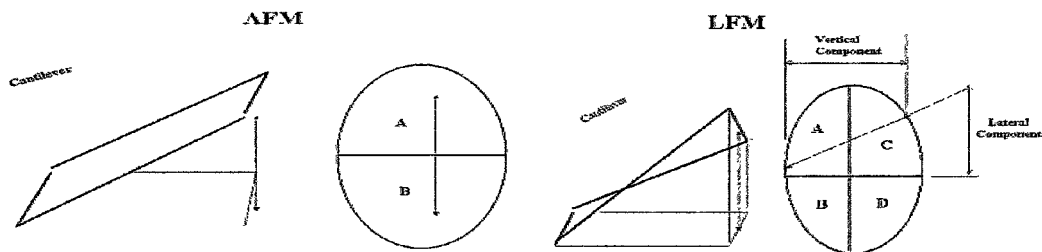


Figure 3.1 The difference in the photodiode detectors for AFM and LFM.

By using an LFM head, the AFM is able to detect not only the vertical motion of the cantilever, but also the twisting or tilting motion. This twisting motion of the cantilever arises from forces parallel to the plane of the sample, which constitute the frictional force

between the sample and tip, and the change in slope. It is possible to tell the change in the material of the sample by looking at the LFM images. As the tip scans through the sample of the same material, the tip would maintain the constant motion. But when the tip begins to scan through the different material, the tip will experience a different friction force and will tilt due to that force.

The LFM mode also detects the change in the slope of a sample. As the tip scans through the features on the sample, the tip will tilt. When the tip goes up the feature the cantilever will tilt in one way, and when it goes down the cantilever will tilt the other way. The Cantilever will maintain the same tilt when it scans through a flat surface. Two cases described above are illustrated below:

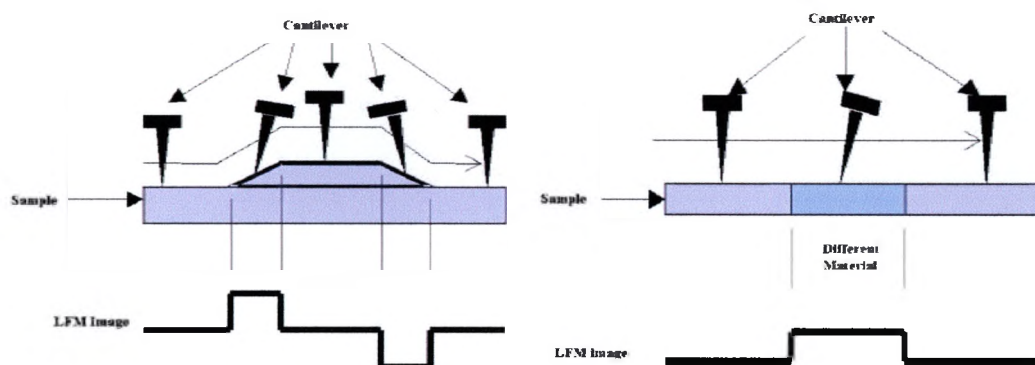


Figure 3.2 Two kinds of LFM deflection: changes in sample feature on the left and changes in friction of the surface on the right.

Because the twisting motion of the cantilever also contains the information about its topography, we see both techniques simultaneously. By comparing the LFM and AFM images, it is possible to separate morphology and composition images.

To focus the laser on the top of the cantilever, three digital voltmeters are used. The first two are the same voltmeters we use for the regular AFM mode. In the LFM photodiode detector, the equation $[(A+C)+(B+D)]$ is used to get the total intensity on the

photodiode detector. The $[(A+C)-(B+D)]$ is used to describe the motion in the vertical motion, where A-B is used for AFM mode. To fix the A-B signal in the LFM, the screw F in Fig.2.2 is used. The tilting motion of the cantilever is monitored by the voltmeter called LFM. The LFM voltmeter, $[(A+B)-(C+D)]$, is used to detect the tilting motion. The screw E in Fig.2.2 is used to set the voltage to $< +/-100\text{mV}$.

Here are some examples of LFM images we have taken. First four images are tungsten film taken with an ultralever. The size of these images are $3\mu\text{m} \times 3\mu\text{m}$. The two on the left are topography (one is a right-to-left direction scan and the other one is a left-to-right direction scan), and the two on the right are LFM images. The second four images are of a copper film taken with the same cantilever as the tungsten images. The size of these images are $1\mu\text{m} \times 1\mu\text{m}$.

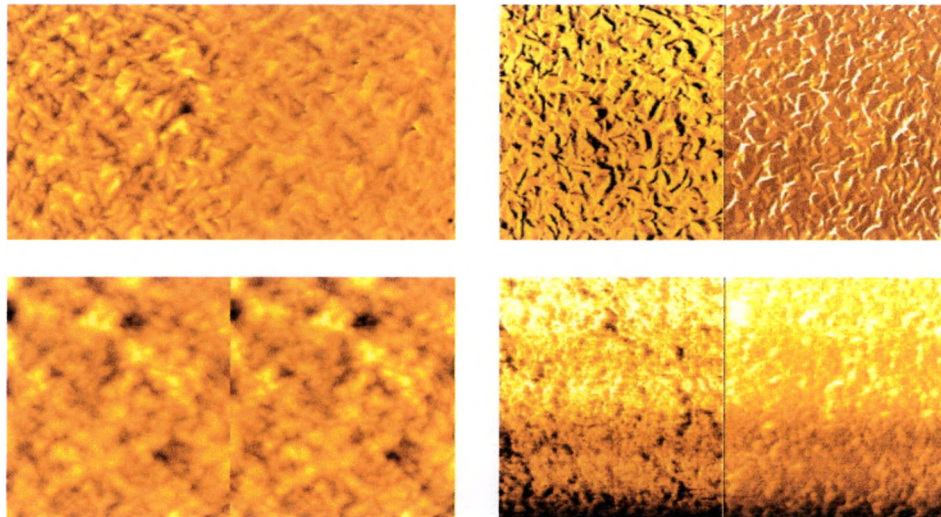


Figure 3.3 Contact AFM images and LFM images of tungsten film on the top and copper on the bottom.

3.1.2 Magnetic Force Microscopy

Magnetic Force Microscopy (MFM) is a useful technique to detect the magnetic force on the sample surface. In this technique, either non-contact mode or intermittent-contact

mode must be used. Also, a tip coated with a ferromagnetic thin film is used. A ferromagnetic material is a material that shows local order of the magnetic spins. The areas where the magnetic spins are parallel are called domains. The magnetostatic interaction between the magnetic tip and the stray field above the sample changes the resonant frequency of the vibrating cantilever. By detecting these changes in the resonant frequency, MFM maps the magnetic domains of a sample. Topographic information of a sample is also contained in MFM images so the topography and MFM images can be imaged simultaneously. How MFM works can be understood by looking the illustration below:

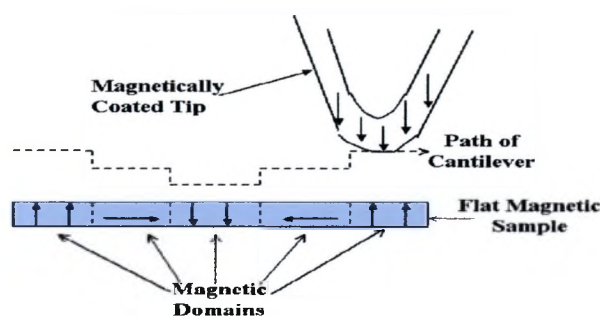


Figure 3.4 The schematic that shows how MFM works. The magnetized tip moves vertically corresponding to the magnetic domains of the sample.

The separation between the tip and the sample determines which information, i.e. topographic or magnetic information dominates. When the tip is further away from the sample than the non-contact regime discussed in section 2.4, the picture will mainly show magnetic feature because the magnetic force varies as $1/r^2$ (long distance) while the van der Waals force varies as $1/r^5$ (short distance)⁴. As the separation decreases, the topographic information begins to dominate. Here are some MFM images of a computer hard drive taken by B. White, E Wittry, and H. Galloway at SWT.

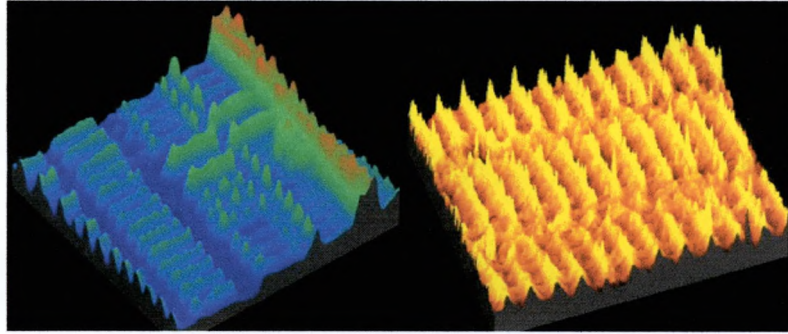


Figure 3.5 MFM images of a computer hard drive taken by B. White, E. Wittry, and H. Galloway at SWT.

3.1.3 Electrostatic Force Microscopy

Electrostatic Force Microscopy (EFM) is very similar to MFM. Like MFM, EFM uses an electrically charged cantilever to scan the sample in the non-contact mode. The difference between these techniques is that the cantilever deflects as the charged domains of the sample changes, instead of magnetic domains in MFM. The motion of the cantilever determines the magnitudes of charge density of the sample. One of EFM's applications is a technique called voltage probing. In this technique, EFM images of an electronic circuit, when a voltage is on and off, are taken to test whether the circuit works properly without any electric leakage.

3.1.4 Force Modulation Microscopy

Elastic characteristics of the sample can be studied using Force Modulation Microscopy (FMM). This technique uses contact mode, but an oscillating voltage is applied to a piezoelectric to move either the cantilever or the sample. Depending on the elastic characteristics of the sample, the cantilever vibrates differently. To keep the deflection of the cantilever constant, a feedback loop is used to move the scanner. This data is recorded to plot the FMM images. Because the vibration of the cantilever is on

the order of hundreds of kilohertz, topographic information of the sample can be distinguished from the cantilever deflection.

3.1.5 Phase Detection Microscopy

Another technique used to study mechanical characteristics like elasticity, adhesion, and friction of a sample is Phase Detection Microscopy (PDM). Either non-contact or intermittent mode is used and a voltage is applied to the piezoelectric or the cantilever in this technique. PDM studies the characteristics of the sample by seeing the lag between the signal applied to the cantilever and the output signal of the vibration changes of the cantilever due to characteristic changes of the sample.

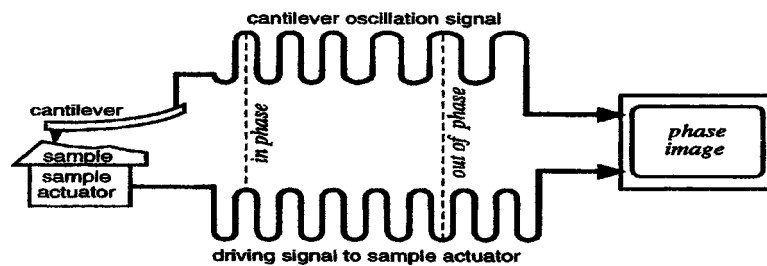


Figure 3.6 There is difference in the phase lag depending on the mechanical characteristics of the sample.

As can be seen in the diagram above, the lag can be detected by checking the point where two signals are in phase and where they are out of phase. For the sample that can be imaged with contact mode, it is better to use FMM because PDM is more complicated than FMM. But PDM must be used to study the mechanical characteristics of the sample that can be destroyed due to tip-and-sample contact.

CHAPTER 4

SCANNING CAPACITANCE MICROSCOPY (SCM)

4.1 Motivation for Scanning Capacitance Microscopy

Scanning Capacitance Microscopy (SCM) is able to detect the dielectric properties of a sample. The capacitance is important in the semiconductor industry because a dielectric is used for memory devices and the ability for memory to be stored accurately depends on the amount of capacitance per unit area. The capacitance of a parallel-plate capacitor can be calculated with the equation:

$$C = \epsilon A/d = k\epsilon_0 A/d \quad \text{Equation 4.1}$$

Where ϵ is the permittivity in the dielectric material, A is the area of the electrodes, d is the separation between the electrodes, k is the dielectric constant, and ϵ_0 is the permittivity of free space (vacuum). To increase the capacitance, the industry could use a material with higher dielectric constant, larger electrodes, and/or smaller separation between the electrodes. Some companies in the industry manufacture complicated shaped capacitors to have bigger areas. The only problem with this idea is the high cost. There is a limitation in the separation distance between the electrodes. Once this is less than $\sim 20\text{-}50\text{\AA}$ in the vacuum, there would be charge leakage in the capacitor. This leakage can be caused by a quantum mechanical phenomenon, in which the electrons tunnel across the barrier between the electrodes. Depending on the material's dielectric

constant, the separation distance can get much shorter. So the only option to maintain a high capacitance per unit area is to use a material with a higher dielectric constant than silicon dioxide (SiO_2).

Also, capacitance is important to the semiconductor industry because increasing the dielectric constant of the gate oxide can increase the speed of an integrated circuit (IC) and also by decreasing the capacitance of space between interconnects. By increasing the dielectric constant of the gate oxide, the thickness of oxide can be reduced while maintaining the same capacitance. Because of the reduction in the thickness of the oxide, less voltage is required to operate transistors. Decreasing the dielectric constant of space between interconnects decreases the time constant. The product of resistance and capacitance has a unit of time. This can be easily understood when we look at the equation for the charging capacitor:

$$q = CV*(1-e^{-t/RC}) \quad i = dq/dt = (V/R)*e^{-t/RC} \quad \text{Equation 4.2}$$

Where q is the charge in a capacitor, C is the capacitance, V is the voltage, t is the time, R is the resistance, and i is the current. Because the exponential value is dimensionless, the product RC must have the same unit as the time. To increase the speed of an IC, the resistance of interconnects must be reduced. Another factor of capacitance in the semiconductor industry is the material used to insulate one component from others. For this purpose, a material with lower dielectric constant is desirable because of the equation below.

$$RC = \rho \epsilon l^2 / td = \rho k \epsilon_0 l^2 / td \quad \text{Equation 4.3}$$

Where R is the resistance, C is the capacitance, ρ is the resistivity, ϵ is the dielectric permittivity, l is the line length, t is the dielectric thickness, d is the line thickness, k is

the dielectric constant of material, and ϵ_0 is the permittivity in vacuum. The product RC is called RC constant. RC constant of the device needs to be reduced because it has units of time. If the value of this constant decreases, the operating speed of components increases. In order to do so, researchers are trying to find new materials with low dielectric constant. SiO_2 has been very common material for this purpose, and it has dielectric constant of 4.2. Now SiOF is common (dielectric constant ranges from 3.8 to 4.2). Researchers are currently looking into materials like polymers (inorganic SiO-C), which have dielectric constant of 2 to 3. In the near future, polymers, porous oxides, and air gap will be researched for this purpose.

For reasons described above, the capacitance is an important factor in the semiconductor industry and needs to be studied. In this chapter, we will discuss how the capacitive characteristic of semiconductor can be studied using AFM.

4.2 Theory of Scanning Capacitance Microscopy (SCM)

To take capacitance images, the AFM must be modified. The following diagram shows how Scanning Capacitance Microscopy (SCM) is set up:

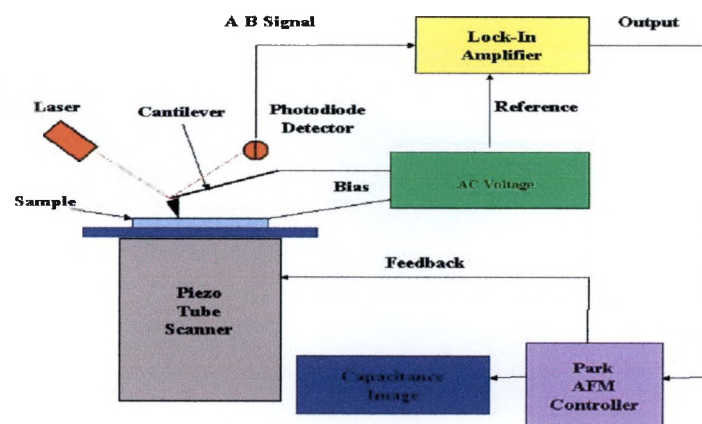


Figure 4.1 Modification on AFM to take SCM images.

The difference between the regular AFM and SCM is that we apply an AC voltage of ~2-3 V, oscillating at the resonant frequency of the cantilever (about 45kHz), between the tip and the electrode of the sample. Corresponding to the capacitive characteristics of the sample the cantilever vibrates differently, and the change in the oscillating frequency is recorded to map the capacitance images. Because the feedback of the AFM can only operate at frequencies <1kHz, we use an instrument called a lock-in amplifier so that we are able to operate the system in the frequency range of about 45kHz. Also, at high frequencies, it does not oscillate the sample. What the lock-in amplifier does is that it measures the amplitude of the signal coming from the AFM at the specific frequency of the AC bias voltage. The lock-in amplifier is basically a narrow band filter that only amplifies a certain frequencies. As the other frequencies are not amplified, noise is suppressed.

The lock-in amplifier could also measure the amplitude of the input signal at twice the frequency of the reference signal. This feature comes out to be useful when the capacitance images are being taken. The energy stored in a capacitor can be calculated by the equation:

$$U = (1/2) * CV^2 \quad \text{Equation 4.4}$$

Where C is the capacitance and V is the voltage applied to a capacitor. The force on capacitance due to this energy is equal to the negative gradient of the energy:

$$F_z = (-\nabla U)_z = (\partial C / \partial z) * (V^2 / 2) \quad \text{Equation 4.5}$$

Where $V = V_0 \sin(\omega t)$ because the voltage applied to the system is AC. So the equation above becomes:

$$F = -(1/2) * (\partial C / \partial z) * (V_0^2 \sin^2(\omega t)) = (1/4) * (\partial C / \partial z) * (V_0^2 (\cos 2\omega t - 1)) \quad \text{Equation 4.6}$$

What we are measuring in SCM images is the force that is proportional to the derivative of the capacitance of the sample. By looking at the equation above, we are able to see why second harmonic is important in SCM. The following plots show the difference in $1f$ (frequency) and $2f$ (two times frequency) when we plot the amplitude versus the frequency ⁷.

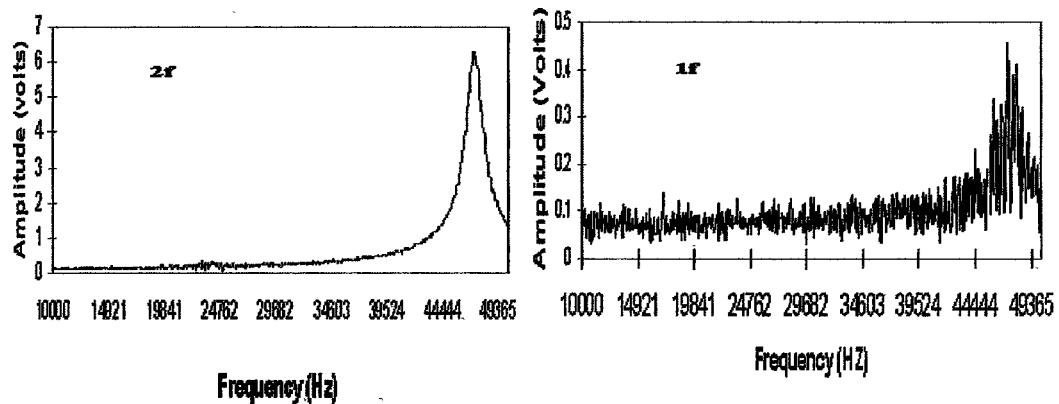


Figure 4.2 The difference in the plots where the amplitude of the signal versus frequency. The plot on the left is $2f$, and $1f$ on the right.

Note magnitude of y-axis is different in these two plots. The plot $2f$ versus amplitude has much higher signal to noise ratio.

For SCM, pickup sensitivity for taking capacitance images is very important parameter. The sensitivity is the ratio of change in diode voltage, v , with respect to the change in the stylus-to-sample capacitance, C_{SS} , and it can be calculated with an equation below:

$$\Delta v / \Delta C_{SS} = (dv/df) * (df/d C_{SS}) \quad \text{Equation 4.7}$$

Where f is the frequency of the resonant circuit. Because a plot for the resonant frequency is in bell shaped, $v = V_P / (1 + (2(f_0 - f)/B)^2)^{1/2}$, where V_P is the detected voltage at maximum value on the bell shaped curve, f is the resonant frequency, f_0 is the drive

frequency, B is the -3dB bandwidth. Then after few assumptions, the equation above can be simplified to:

$$\Delta v / \Delta C_{SS} = \alpha * (\gamma / C) * (V_p f / B) \quad \text{Equation 4.8}$$

Where α is the constant of proportionality and is equal to $(3)^{1/2}/4$, γ is a coefficient of frequency sensitivity, and C is the total capacitance. By looking at this equation, increasing the sensitivity for capacitance detector can be achieved by applying high drive voltage and operating at a high frequency ⁸.

The carrier-to-noise (CNR) ratio is also important factor for increasing the pickup sensitivity. This ratio can be expressed by:

$$\text{CNR} = \Delta v / (n_s^2 + n_c^2)^{1/2} = (\Delta v / n_s) / (1 + (n_c / n_s)^2)^{1/2} \quad \text{Equation 4.9}$$

Where Δv is the output carrier level, n_s is the noise originating in the sample, n_c is the noise generated in the pickup circuit ⁸.

Because the lock-in amplifier in our lab can only detect up to 100kHz and the fact that second harmonic is used, there is a limitation of tips that we are able to use in the experiments. The limitation is that the cantilever cannot have a resonant frequency over 50kHz . Also, we must use Ultralevers or cantilevers that are coated with a conductive material so that a voltage can be applied over the tip and the electrode of the sample.

4.3 Data

The first experiment we did with the SCM was to do a capacitance analysis of a sample given by Motorola. The sample is 600\AA Barium Strontium Titanate (BST) laid on 1000\AA platinum, which is laid on 4000\AA of oxide. All of these materials were grown on a silicon wafer. To understand the capacitive characteristic of the sample, we did four

different analyses. These experiments are capacitance as a function of voltage, set point, frequency, and position on the wafer. These experiments are the subject of this section.

4.3.1 Capacitance as a Function of Voltage

In this experiment, we kept all parameters constant except the voltage we applied to the tip and the sample. We varied the voltage from 0.1V to 5.0V by every 0.5V. We started to take data at 0.1V because there is not any capacitance when zero voltage is applied. For each voltage, we took three images so that we were able to take average of height. Starting at the data for 4V, we had to change the sensitivity of the lock-in amplifier. For each voltage, we took three images so that we were able to take average of height. The following is the data we got from this experiment.

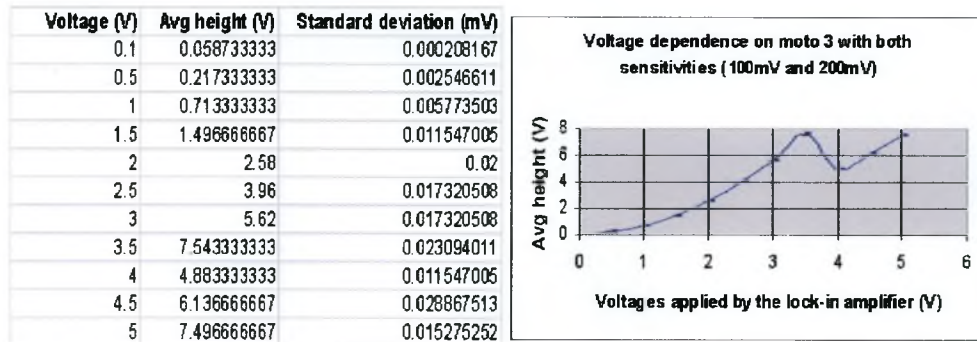


Figure 4.3 Voltage dependence on Moto 3 with both sensitivities (100mV and 200mV)

As can be seen on the graph, there is a big drop at 4V. At first, we were not sure what caused this drop. But we concluded that this was caused by the change of sensitivity. So we then plotted a graph with the sensitivity of 100mV, and we also plotted a graph with sensitivity of 200mV separately. The results for the sensitivity of 100mV and 200mV follow:

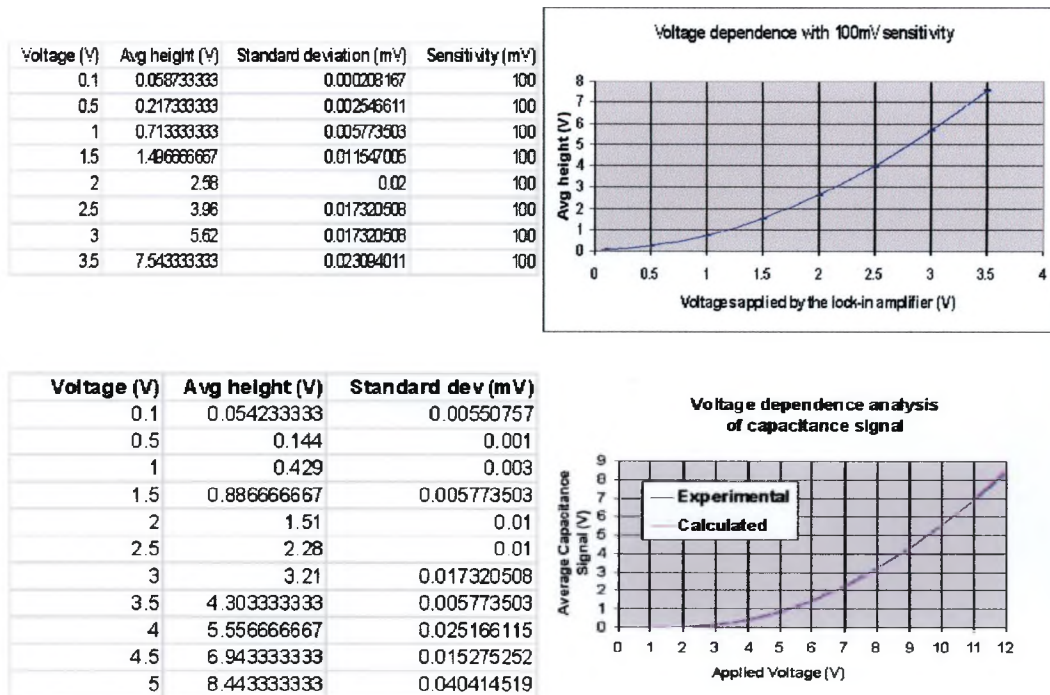


Figure 4.4 Voltage dependence with 100mV sensitivity on the top, and voltage dependence analysis of capacitance signal.

The second graph (sensitivity of 200mV) also includes both experimental and calculated data. We assumed by that these graphs are in a function of square of voltage ($y=A*x^2$ where A is a constant). So what we did for calculated data was to subtract the calculated value from the experiment value for each voltage and square the value. The number at the right bottom corner is the sum of all these values. We did this because we wanted to calculate χ to fit the curve with a following equation:

$$\chi^2 = \sum_i [(y_i^{\text{th}} - y_i^{\text{exp}})^2 / \sigma_i^2] \quad \text{Equation 4.10}$$

Where y_i^{th} is the theoretical value, y_i^{exp} is the experimental value, and σ_i is the standard deviation for each data. What we did was to get the largest χ for using a second power function by varying the constant A and compare the value with the smallest χ value for different power function. The largest value of χ^2 for second power function we

calculated was 4539.44. The smallest value for χ^2 that we got for third power function was 74161.1. The smaller the number is, the graph is more fitted so that we can say that the second power function is more fitted than other power functions.

4.3.2 Capacitance as a Function of Set Point

We then varied the value of set point and kept other parameters constant. As we explained in chapter 2, the set point controls the amount of the bending of the cantilever. First, we varied the set point every 10nN from -20nN to 50nN and plotted the corresponding average height. Because the cantilever we were using broke, we began to take images with new tip at 40nN. All of the data we got was from $1\mu\text{m} \times 1\mu\text{m}$ images. The following table lists the results we got from this experiment:

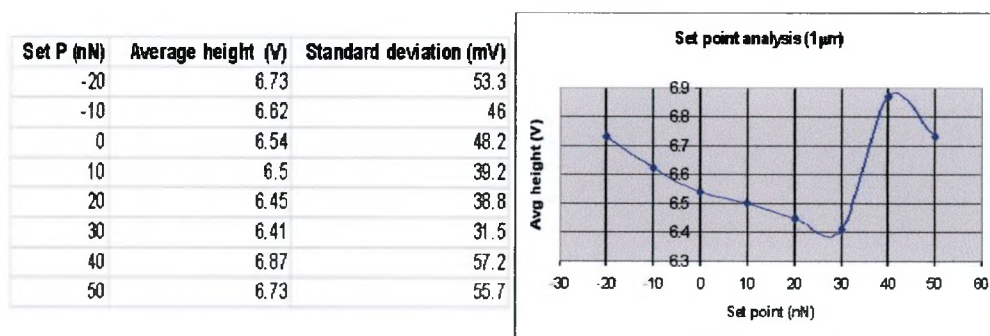


Figure 4.5 Set point analysis of Moto 3.

Because a new tip is used, the graph increases dramatically at 40nN. Next, we used a brand new tip and did the experiment. These images are taken at $0.5\mu\text{m} \times 0.5\mu\text{m}$ size. The results follow:

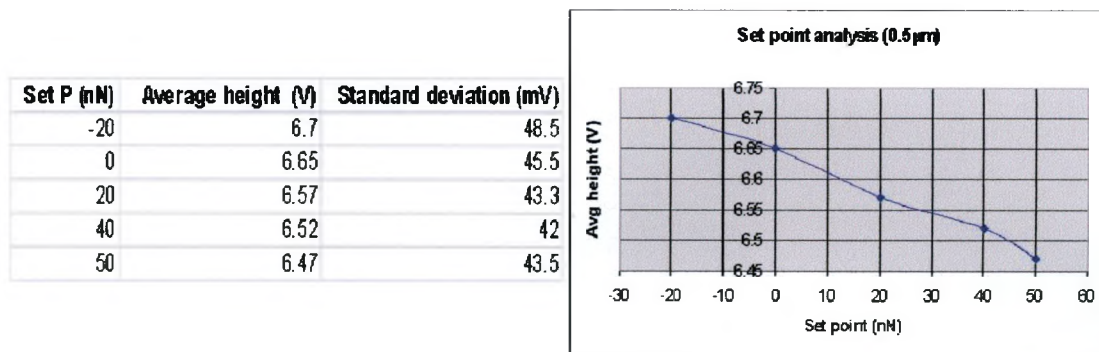


Figure 4.6 Set point analysis (0.5 μ m)

As we see the results, we conclude that as the set point increases, the force between the tip and the sample also increases. So this experiment makes sense because if the tip is pressed hardly against the sample, the tip is not able to vibrate as much as it wants to. These graphs seem to be linear.

4.3.3 Capacitance as a Function of Frequency

In this experiment, we first picked the resonance frequency using the non-contact clock. What this technique does is that a computer applies the voltage with different frequencies to the cantilever and detects the frequency with the highest oscillation. This technique is used when non-contact mode is used. The cantilever we used for this experiment had its resonant frequency at around 45.35kHz. What we were interested in was how capacitance signal depends on the frequency of a voltage applied to the tip and the electrode of a sample. We selected the resonant frequency and +/-0.25V, +/-0.5V, +/-1.0V, and -1.5kHz of the resonant frequency to take data. We took five images for each frequency and calculated the averaged capacitance signal. The data for this experiment follows:

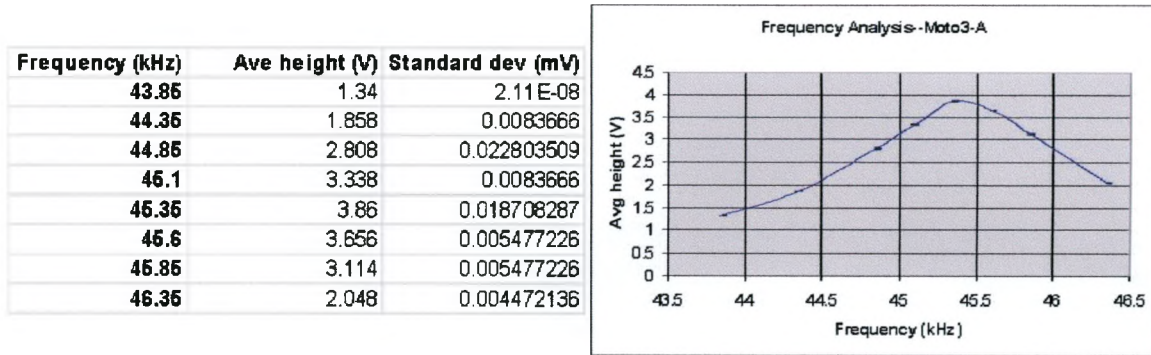


Figure 4.7 Frequency analysis of Moto3-A

The results that we have are consistent with the theory. Theoretically at the resonant frequency, the highest average capacitance signal is detected. As the frequency goes over the resonant frequency, the capacitance signal begins to decrease. One thing that we do not understand is that, above the resonant frequency, the SCM images invert in the respect of the images before the resonant frequency. Here is an example of this phenomenon.

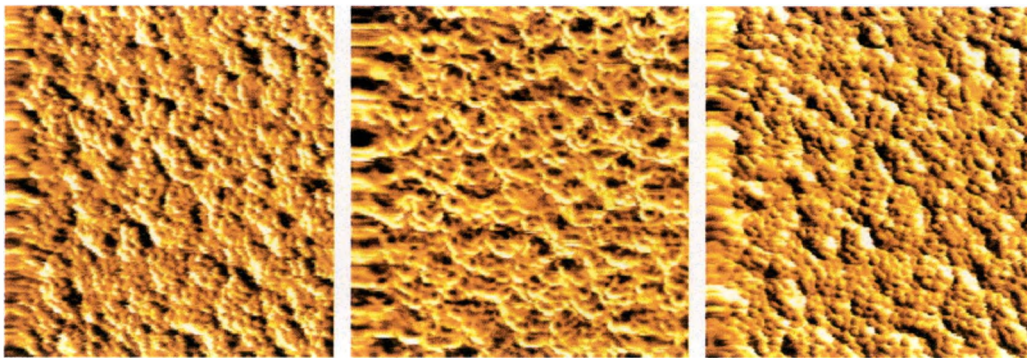


Figure 4.8 SCM images of Moto3 at different frequencies (from left 44.35kHz, 45.35kHz, and 46.35kHz).

An image in the middle was taken at the resonant frequency of the cantilever, 45.35kHz. One on left was at 44.35kHz less than the resonant frequency, and one on right was at 46.35kHz. As can be seen on the images, the one on right seems to be inverted in the respect of two images on left.

4.3.4 Capacitance as a Function of Position on the Wafer

When the sample was given to us, Sufi Zafar at Motorola told us that the sample has a variation in the dielectric constant from the center to the edge. The dielectric constant is about 40% higher in the center with respect to an edge point. To verify, we cut the wafer into four little pieces; from the center of it to the edge as shown in the diagram below:

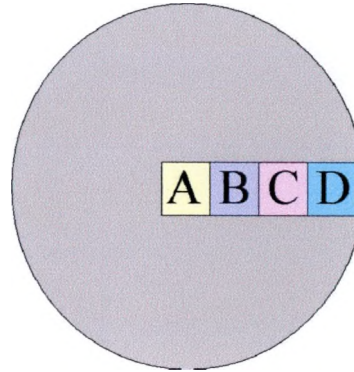


Figure 4.9 How the wafer was cut into pieces A, B, C, and D.

For each piece, we took ten SCM images and averaged the capacitance signals to see whether there is 40% difference. The data we got follows:

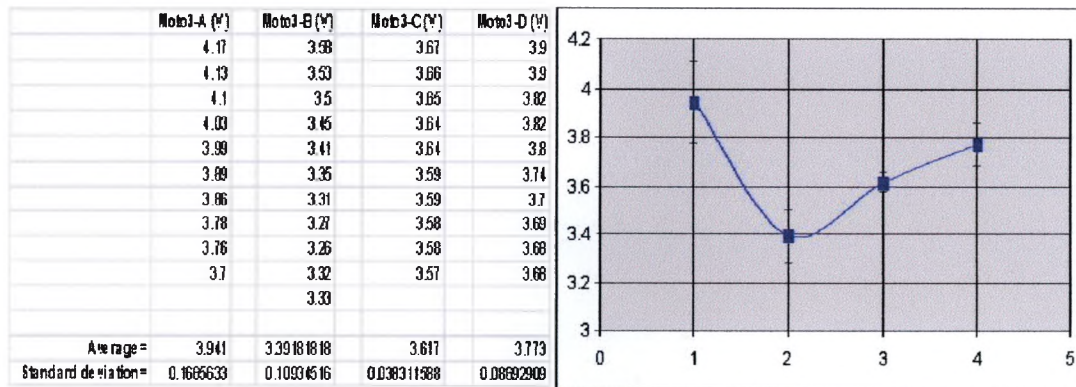


Figure 4.10 Plot of average heights at each section.

By looking at the data and graph above, our result is not consistent with what Zafar told us how it is.

4.4 Non-Contact SCM

We are able to take capacitance images with AFM's non-contact mode. This technique is called non-contact SCM. This technique is used when you do not want to have any friction forces between the tip and sample or when the material is too soft for contact mode. What we do is that we first approach the cantilever to the sample by a regular non-contact AFM method. After completing the approach, we applied AC voltage between the tip and sample as we do in regular SCM technique. But in non-contact SCM, we usually apply little bit more voltage because of the separation between the electrodes. Here are examples of non-contact SCM. The sample is the same one we used in the experiments in the previous section.

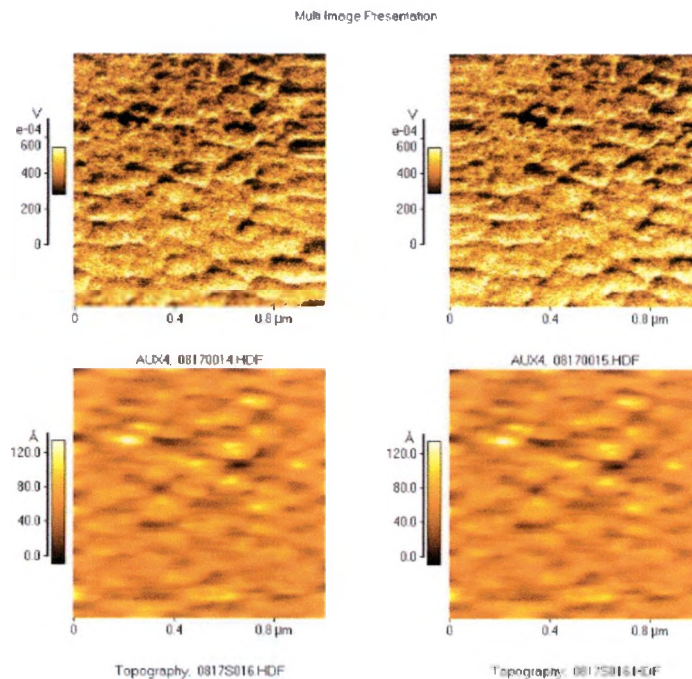


Figure 4.11 Topography and non-contact SCM images of Moto3.

When the regular SCM images are compared with non-contact SCM images, it is clear that non-contact SCM images have lower resolution. There is also a technique called tapping mode capacitance microscopy where the tip sometimes makes contact with the

sample while it is vibrating off the sample. This technique gives better resolution compared to the non-contact SCM, but less resolution than contact SCM.

4.5 RCA VideoDisk Technique

In late 1970s, researchers used the capacitance pickup device from RCA VideoDisk to take capacitance images. RCA VideoDisk reads signals from a disk, which contains video and audio information. The stored information is read by measuring the capacitance between the stylus and disk as the stylus is guided through a fine spiral groove on the disk. To store and detect capacitance as a signal, the disk must be conductive or must have a conductive layer on the disk. One of the advantages of using RCA VideoDisk is that it can detect capacitance as small as 10^{-4} pF^{8,9}. Another advantage is that, because it can resolve the signal elements much smaller than the wavelength of light, it is very reliable to reproduce high quality signals.

The stylus used in this system is made of diamond and sapphire. Electrode is coated on the trailing face of the stylus. The stylus tracks the groove on the disk with its triangular shape. The thickness of electrode ranges from 1000-1500Å⁹. The diagrams that describe how stylus and disk interact follow:

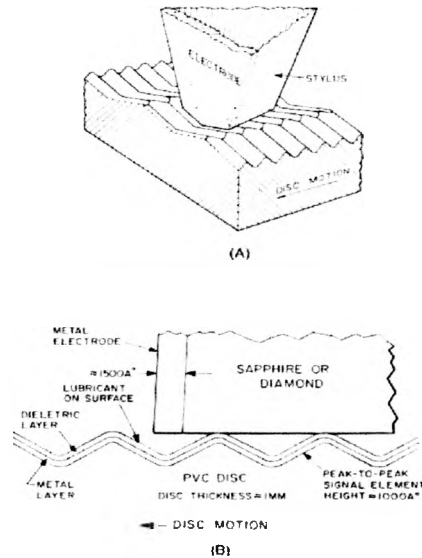


Figure 4.12 Perspective and cutaway views of stylus and coated disc 9,10.

The following diagram explains how capacitance between the stylus and disk is measured when pickup circuit is operating at 915MHz:

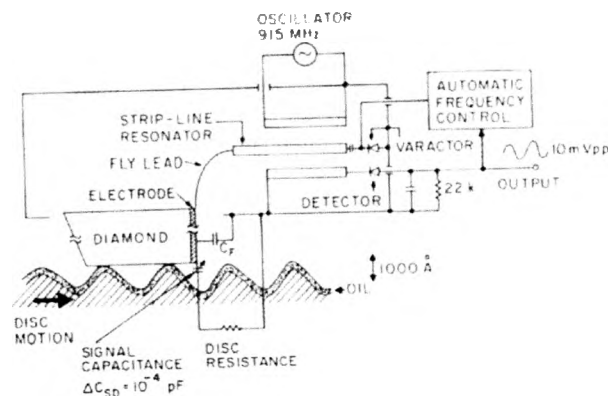


Figure 4.13 How SCM with a transmission-line pickup circuit is set up 8.

For taking capacitance images of thin films, a cantilever of the AFM can be used as a stylus. Also, the electrode of the sample must be connected to the system. By doing so, capacitance can be measured as a cantilever probes the sample. Using RCA VideoDisk capacitance pickup sensor, p-n junction analysis can be done 11-14.

The disadvantage of this system is that it is very difficult to find this device. It has been more than 20 years since RCA VideoDisk was produced. Only few companies handle parts for it.

CHAPTER 5

LIQUID CELL

5.1 Theory of Microcell

Liquid cell is a technique used to take AFM images of a solid surface covered by a liquid using the component called microcell, shown below.

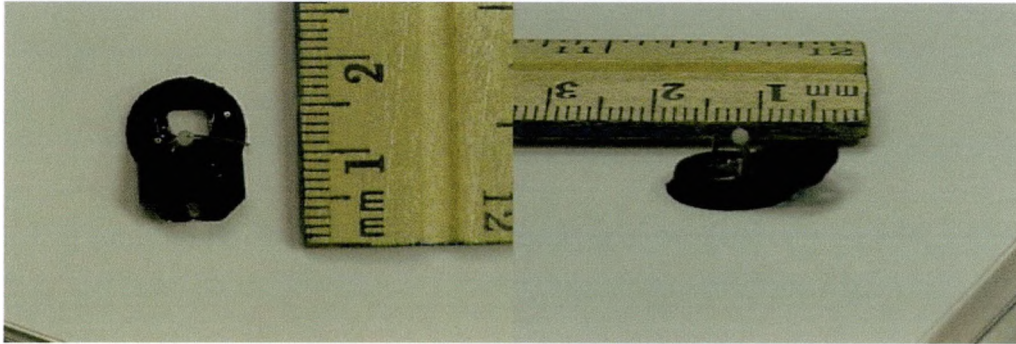


Figure 5.1 Top and side views of a microcell.

The basic concept of this technique is to insert liquid into the space between the microcell and the sample. Instead of spotting the laser beam on the cantilever directly as in a regular AFM, the laser beam must pass through the window (glass) on the microcell and through the liquid in the microcell before hitting the cantilever. Because of the refraction at each interface, it is very difficult to reflect the laser off the top of the cantilever and to catch the reflected laser beam on the photodiode detector.

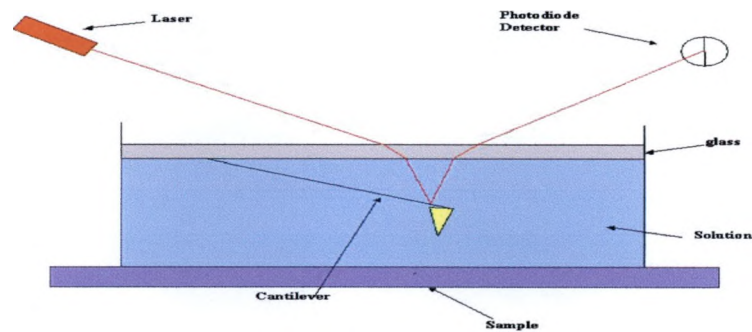


Figure 5.2 The diagram that shows how liquid cell works, and it shows that the laser beam must pass through a glass window and liquid before hitting the top of the cantilever. The laser beam then must pass through the liquid and a glass window again to the photodiode detector.

5.1.1 Modifications

A problem we had with the system shown above was that this microcell was manufactured for use with water or any liquid with high surface tension. When we used a solution with low surface tension, the liquid tended to leak out from the sides of the microcell. This is why we needed to redesign the microcell. Our idea was to construct a tub to hold the liquid. Teflon was chosen to make a tub because it does not react with many solutions, is easy to machine, and because of its availability. We machined a piece of Teflon (2cm x 2cm x 0.4cm) to create a tub space of 1.7cm x 1.7cm x 0.2cm. This size was chosen so that AFM head can properly approach the sample. A sample must be smaller than the tub and is placed inside of this tub. Our idea was to use a regular AFM cantilever and a cantilever holder and operate as in regular AFM.

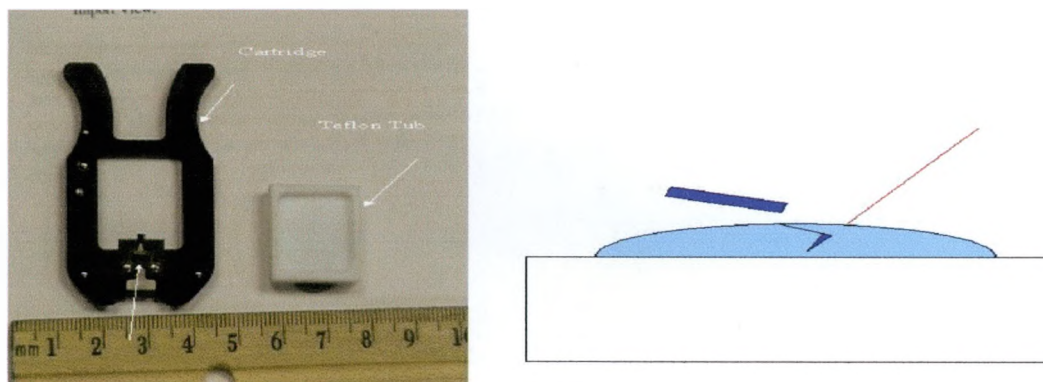


Figure 5.3 The liquid cell technique using the regular cantilever holder and a tub that is made out of Teflon. The sample is set inside of the tub before the liquid is inserted into the tub.

The problem with this system was that it was very difficult to spot the laser on the cantilever and back to the photodiode detector because of the curved surface that the liquid makes due to its surface tension. Again, we had to come up with a new design.

Our next idea was to use a Teflon tub and the microcell at the same time. By doing so, the window on the microcell makes the top of the liquid flat and allows us to easily spot the laser on top of the cantilever.

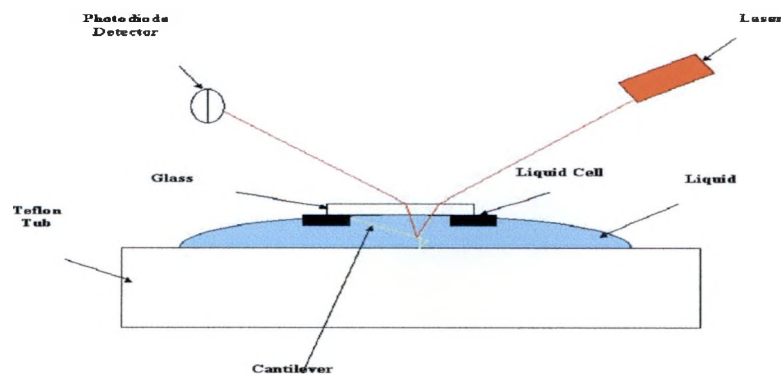


Figure 5.4 The liquid cell system using both the Teflon tub and microcell. This system makes the top of the liquid flat so that spotting the laser beam is easier.

Because Teflon has a high thermal expansion coefficient, we need to make a tub with a material called Kel-F. It is a homopolymer of chlorotrifluoroethylene that has excellent thermal characteristics and maintains an operating temperature range of -400F to 400F .

It also has the lowest vapor transmission rate of any plastic. Another improvement we will use is to use a pump to flow liquid in and out the tub to keep the temperature of the system constant. The flow rate is very crucial. If the flow rate were too fast, it would be the source of noise when images are taken. If the flow rate were too slow, images would have thermal drift. Another reason for the pump is to change pH of the solution while images are taken to see whether pH of the solution affect the imaging or not. The following diagram shows the design with a pump.

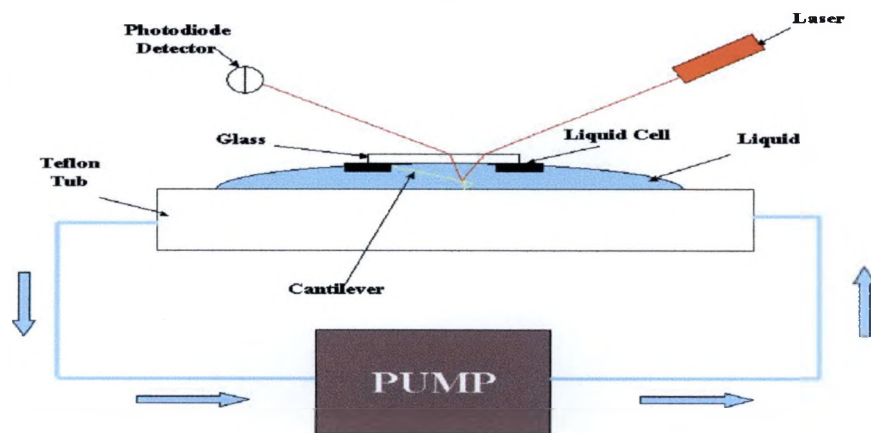


Figure 5.5 The liquid cell with a pump is designed to flow the liquid to keep the temperature of the liquid constant. Another reason we designed this system is to vary the pH of the solution to see the variation in the features on the sample.

The last modification was to use only a few drops of solution. Using a syringe, a few drops of the solution are dropped onto the microcell. Although the surface tension of the liquid is not high, the liquid would stay on the microcell even if the microcell were flipped.

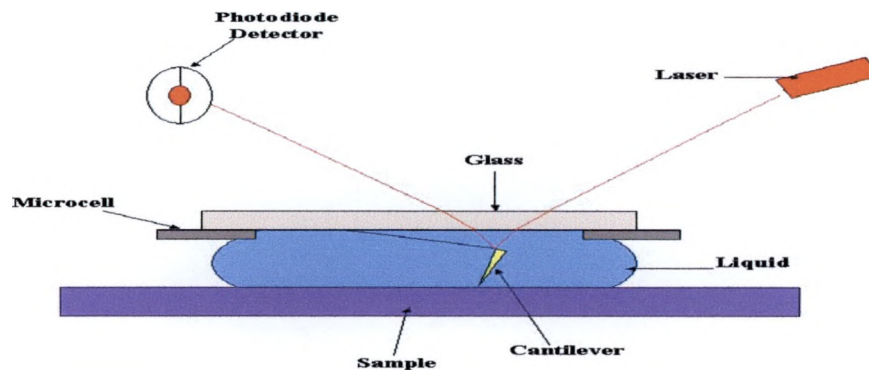


Figure 5.6 The liquid cell system using only few drops of the solution.

The advantage of this technique is that a smaller amount of liquid is required to do the experiments.

5.1.2 Operation of Microcell

Operation of microcell is very similar to that of regular AFM. First, the cantilever chip must be mounted into the microcell. There is a spring that holds the cantilever chip tight to the microcell. This spring needs to be pushed from the other side to insert the cantilever chip. Once this is done, the microcell is mounted on the regular cartridge used in the AFM. Before inserting it into the head of AFM, a few drops of the solution is dropped to the microcell. We then insert the cartridge with the microcell into the AFM. Three screws on AFM head can be used to make sure that the cartridge is held tight to the AFM. This needs to be done because any unwanted movement can cause mechanical noise. At this point, we need to focus the laser on top of the cantilever as we do in the regular AFM and make sure that the A+B signal is higher than 1V (much lower voltage when compared to that of regular AFM) and the A-B signal is as low as possible. We then wait until the solution reaches the room temperature, and the A-B signal settles down. When the A-B signal is settled, we need to lower the head until the solution hits the sample, but not the tip in the microcell to avoid the breakage of the tip. Once the

liquid hits the sample, the A-B signal needs to be set near 0V (<200mV) again because the cantilever is slightly pushed upward due to the contact. The AFM head can then approach the sample automatically as in the regular AFM. The parameter “Gain” represents how fast the feedback of the AFM reacts to the change in features on the sample. It is very crucial not to have noise in the liquid cell because the noise affects not only the cantilever and other AFM components, but also the liquid.

5.1.3 Window Replacement

When we used isopropanol as a solution, it dissolved the glue that holds the window of microcell to the microcell. We had few replacements, but we found out that we needed to use ultraviolet (UV) curing glue. Because we did not have an UV gun available, we had to design the curing system with an UV source (mercury vapor lamp) we found in the storage room. The UV source was converged with a convex lens at the focal length of the lens as shown below:

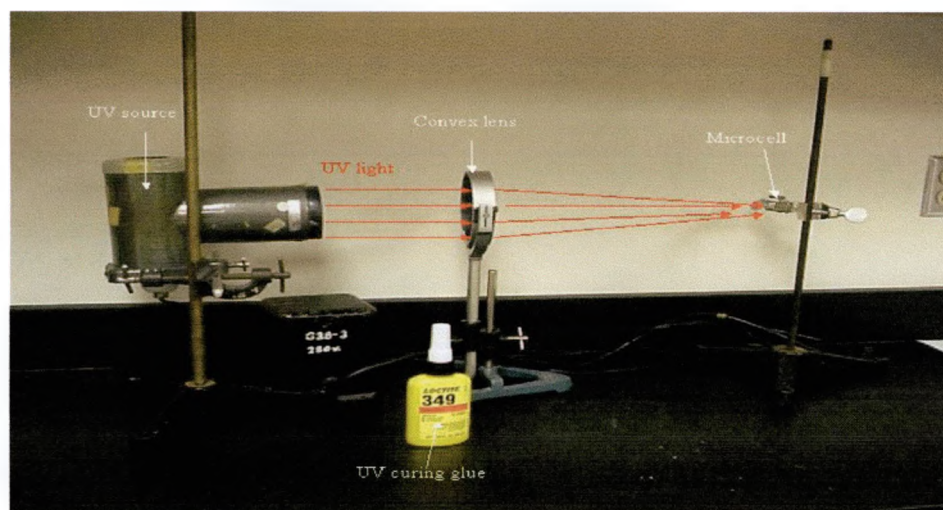


Figure 5.7 UV curing glue is used to replace the window on the microcell. The microcell is set at the point where UV light is converged, the focal point of the convex lens.

Although a UV gun with certain intensity would take only few minutes to cure the glue, our UV source took about 3 hours to cure because of its weak intensity.

5.2 Chemical Mechanical Polishing (CMP)

Chemical Mechanical Polishing (CMP) is the process used in the microelectronic industry to make the surface of the wafers flatter and smoother. As the name implies, it polishes both chemically and mechanically. CMP has become an important process in the industry as the number of layers used in the microelectronic fabrication process has increased as well as due to the decreasing tolerance in depth of focus of the light sources used to create smaller features. The flatter the surface of a wafer is, the more layers can be deposited. Tungsten and copper were two materials that we are interested because tungsten has been the most common used material for the plugs and copper as interconnects in the microelectronic fabrication. So it is required to understand how these materials are actually polished by the CMP process. In this section, we will discuss how CMP works.

A CMP system consists of a wafer located on a polishing head, a slurry with abrasive particles and corrosion inhibitor, and a polishing pad placed on a polishing plate. The wafer and the polishing pad actually make contact. Both a polishing head (wafer attached) and a polishing plate (polishing pad attached) rotate in the same direction while pressure is applied on a polishing head. Slurry is also poured between the wafer and polishing pad. There are abrasive particles in the slurry as stated above. These abrasive particles polish mechanically. Chemical and abrasive particles used in CMP are determined depending on which material must be polished. The polishing pad is there for

the same reason there is a paper for sandpaper. The diagrams below show how CMP works:

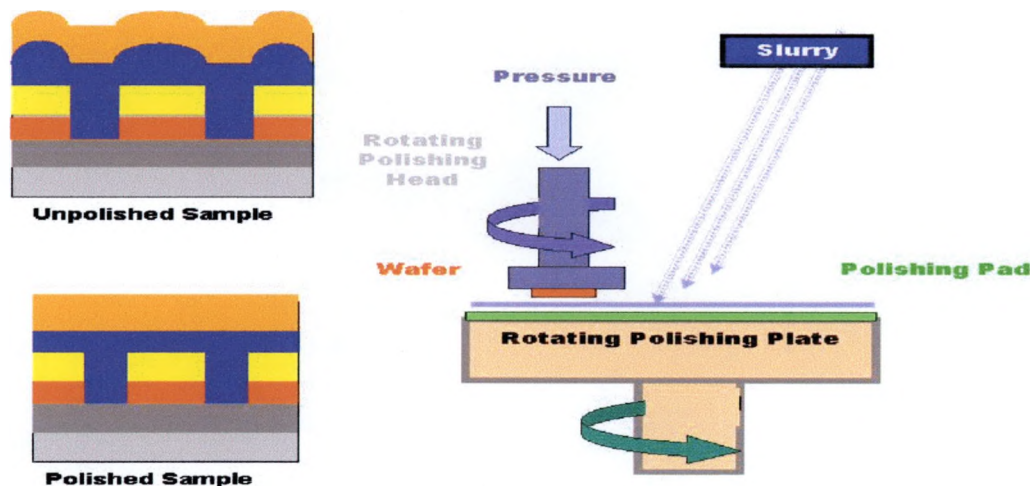


Figure 5.8 The figures on the left show how the unpolished sample differs from the polished sample. The figure on the right shows how CMP process works. The slurry, which consists of the chemical solution, corrosion inhibitor, and abrasive particles, is poured onto the surface of a polishing pad. Both the wafer and polishing pad rotate in the same direction with pressure applied to them.

5.3 CMP Simulation at the Atomic Scale Using AFM

My main project was to simulate the CMP process at the atomic scale using AFM. To understand how this works, the following diagrams are helpful.

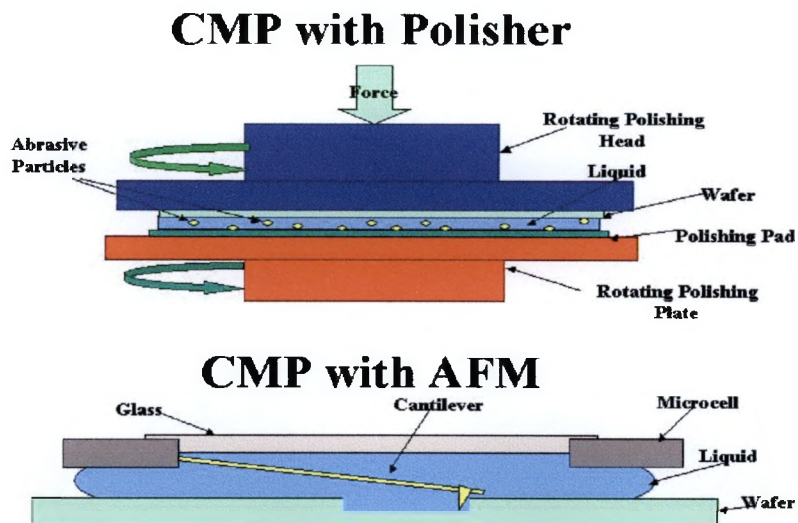


Figure 5.9 The figure on the top shows how CMP with a polisher works. The figure on the bottom shows how we simulate the CMP process with AFM. Everything is pretty much the same except the tip of the cantilever is used as the abrasive particles in the CMP process with a polisher.

The diagram on the top describes how the CMP process occurs in a polisher. Wherever abrasive particles make contact with a wafer with a layer of corrosion inhibitor molecules on top of it, the CMP process takes place. To simulate this with the AFM, we used the cantilever and the tip of the same material as the abrasive particles in the polisher. Also, the chemical solution we used was the same as some of the constituents of commercial slurry. The microcell was used to keep the solution when the images were taken. All the area covered by the microcell was exposed to the chemical. But only in the area where images are actually taken does the tip make contact with the sample. In other words, this is the area that is exposed to the chemical and mechanically scratched by the tip on the cantilever. Ideally, what we hope to see is a “hole” at the area where the tip actually makes contact with the sample.

5.4 Experiments

5.4.1 Samples, Chemicals, and Abrasive Particles

There are many different combinations of chemicals and abrasive particles to smooth surface of certain material. Tungsten and copper are our two interests of material to be removed by CMP process because they are processed by CMP in the microelectronic fabrication industry. Here are a few combinations of the material, the chemicals, and the abrasive particles used in industry.

Table 5.1 Combinations of material, chemical, and abrasive particles used in CMP process in the microfabrication industry. We tried these combinations to simulate the CMP process at the atomic scale ¹⁵.

Material	Chemical	Abrasive Particles
Tungsten	Hydrogen Peroxide (H ₂ O ₂)	Alumina (Al ₂ O ₃)
Tungsten	Potassium Iodate (KIO ₃)	Alumina (Al ₂ O ₃)
Copper	Hydrogen Peroxide (H ₂ O ₂)	Alumina (Al ₂ O ₃)
Copper	Nitric Acid (HNO ₃)	Silica (SiO ₂)

Because hydrogen peroxide can be used for both metals, I started with hydrogen peroxide. The problem we had with this solution is that it oxidizes very easily creating bubbles inside of the solution. It is very crucial not to have bubbles in the microcell because the bubbles are not able to get out from the microcell and are stuck there. This is a problem because AFM uses a laser to map the topography of the sample. The bubbles interfere the path of the laser beam, either the laser beam does not reach to the top of the cantilever or the reflected laser beam off the cantilever does not reach the photodiode detector. The following diagram and picture show this problem in the microcell.

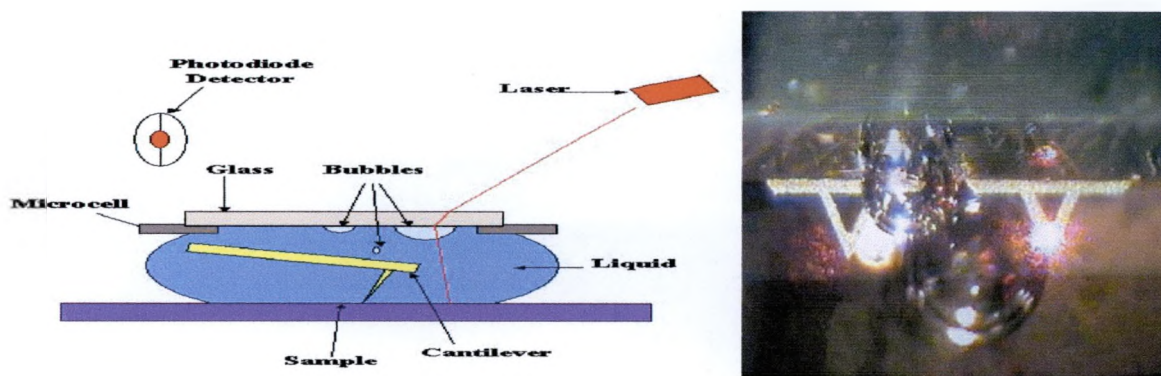


Figure 5.10 These diagram and picture show how bubbles inside of the liquid cell affects the path of the laser beam.

I then tried potassium iodate, but this solution had a thermal drift problem. Thermal drift occurs because of the change in temperature. As the temperature inside the microcell changes the size of cantilever also changes. Because of this, the A-B signal is not stable.

5.4.2 Copper with HNO₃ (0.063%) without Benzotriazole (BTA) and a Silica Tip

Because of the reasons stated in the previous section, we chose to use nitric acid on a copper film with a silica tip. We did not use the corrosion inhibitor, benzotriazole (BTA), in this experiment. What we were looking for was the change in the grain features as images was taken. We took images at an area of $1\mu\text{m} \times 1\mu\text{m}$, and at 2Hz. There are 256 data points in both x and y directions. At a line scan of 2Hz, it takes 1 second to image 2 lines of the whole image. So it takes 178 seconds to take an image at 2Hz. The set point for the cantilever (approximate force between the tip and the sample) was 5nN. Here are the images taken with the parameters described above.

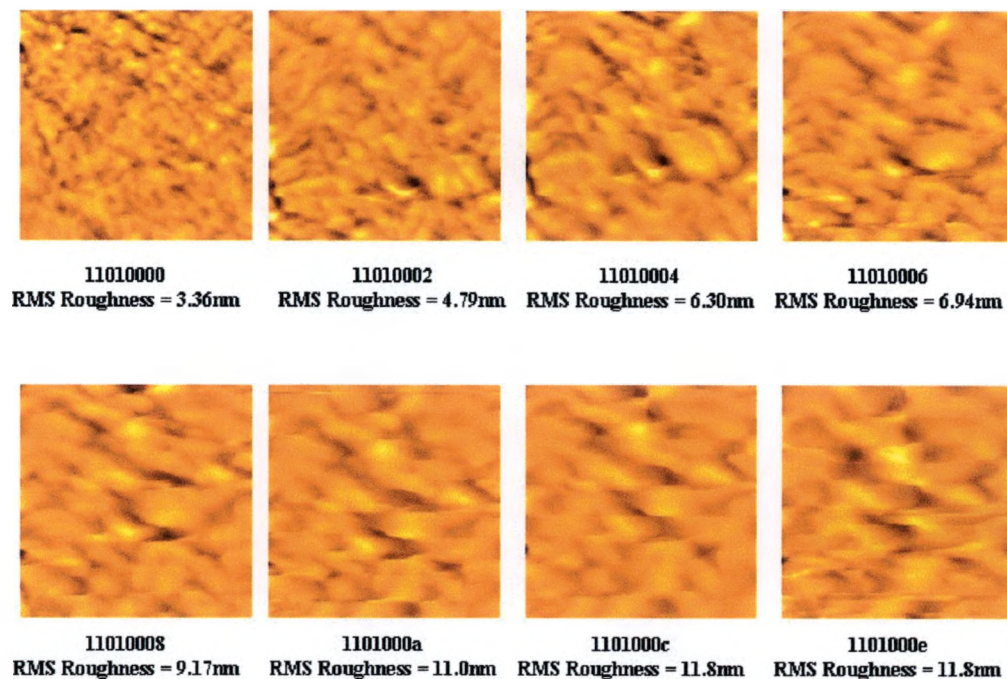


Figure 5.11 The liquid cell images of copper with nitric acid (HNO_3) as the chemical. As shown in the images, the features on the sample surely changed. Each image took about two minutes to be imaged.

As can be seen in the images above, the features of the grains change dramatically as 8 images were taken. We believe that this is caused because we did not mix the corrosion inhibitor in the solution. To see what was going on in this area, we decided to take a bigger image with a $1\mu\text{m} \times 1\mu\text{m}$ area that we took images of at the center. First, we took images at $4\mu\text{m} \times 4\mu\text{m}$, and then at $3\mu\text{m} \times 3\mu\text{m}$. The following diagrams show what happened.

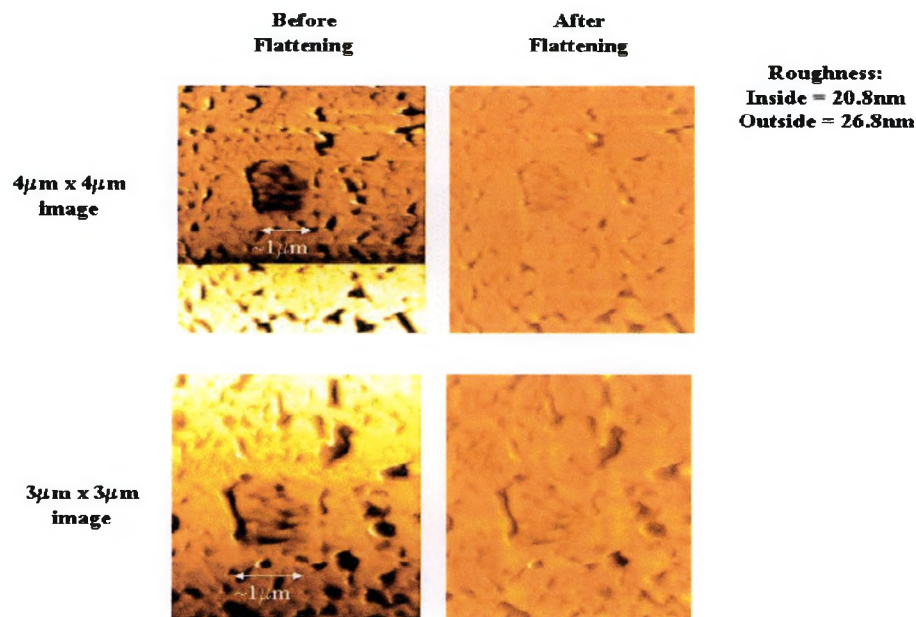


Figure 5.12 The images which were taken after $1\mu\text{m}\times 1\mu\text{m}$ images. Ones on the top are $4\mu\text{m}\times 4\mu\text{m}$ images and ones on bottom are $3\mu\text{m}\times 3\mu\text{m}$ images. In both sizes, almost perfect square of $1\mu\text{m}\times 1\mu\text{m}$ can be seen where we took $1\mu\text{m}\times 1\mu\text{m}$ images earlier. Two images on right are images that were flattened by the software.

Two images on the left are images before images were corrected by software to fix the nonlinearity. And two on right were after the correction. As can be seen in the images, there is about a $1\mu\text{m}\times 1\mu\text{m}$ square located at about the center of each image. This proves that the area that was scratched and exposed to chemical is polished more than elsewhere. The area that was scratched was about 500\AA deep. Because we took 8 images at $1\mu\text{m}\times 1\mu\text{m}$, it scratched off 62.5\AA per image. As I stated above, the roughness is high compared to the previous experiment because we did not use the corrosion inhibitor.

5.4.3 Copper with HNO_3 (0.063%) with BTA and Silica Tip

The whole purpose of the CMP process is to make the surface of the sample flat and smooth. As we saw in the previous subsection, we do not want the roughness to increase.

To see if BTA affects the roughness of the sample, we mix BTA with the same solution we used for the earlier experiment. What we believe BTA does is that, as soon as the solution makes contact with the sample, a monolayer of BTA molecules are laid on top of the sample. BTA molecules protect the sample from the chemical. The BTA molecules are removed from the area where the tip makes contact with the sample. Only this area is exposed to the chemical, and the CMP process occurs. But as soon as tip moves away from the area, another monolayer of BTA molecules is laid and protects the sample. The diagrams below illustrate this process.

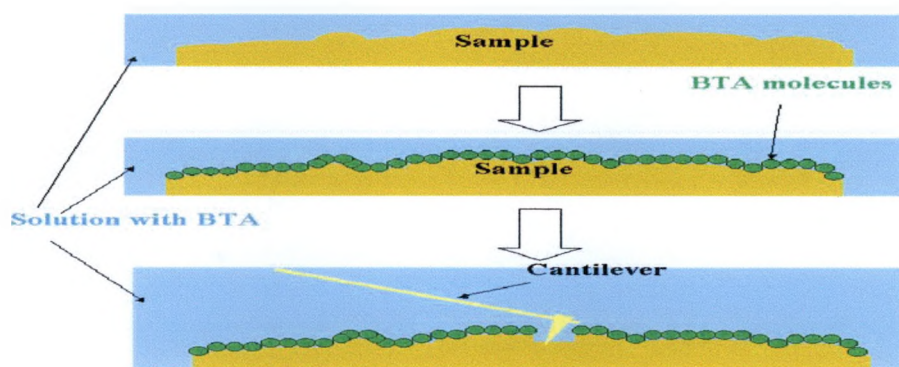


Figure 5.13 These diagrams show how the solution with corrosion inhibitor like BTA would create a monolayer on top of the sample. When the solution with BTA makes contact with the sample, the monolayer of BTA molecules is laid. Only the area the tip on the cantilever makes contact is where CMP process occurs.

The parameters we used for this experiment were a set point of 136.5nN and scan frequency of 2Hz. Again we started to take images at $1\mu\text{m}\times 1\mu\text{m}$ and took eight images. The results are shown below.

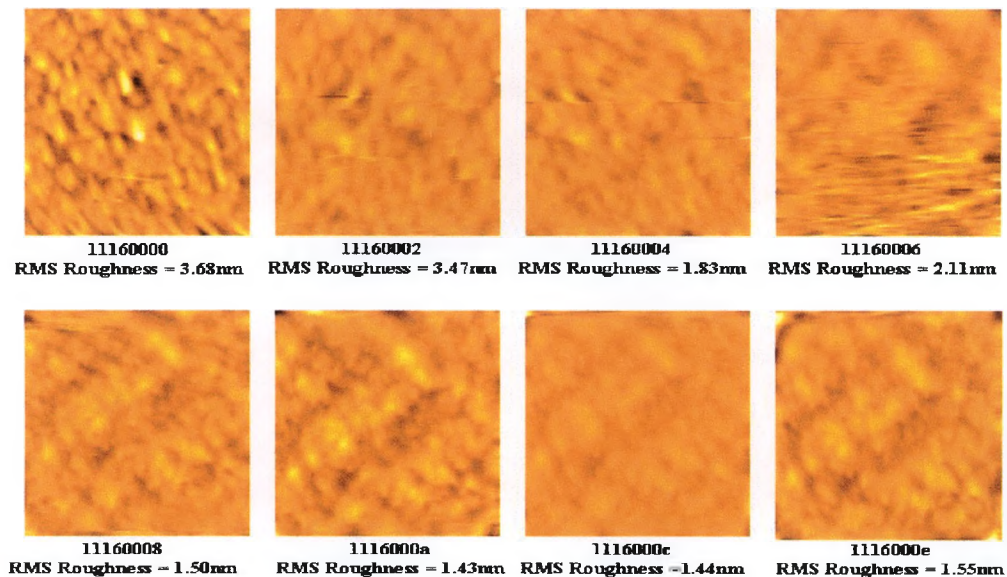


Figure 5.14 The liquid cell images of copper with nitric acid (HNO_3) with BTA. Once again the features on the sample changed. Also, the RMS roughness of images decreased as more images are taken. Each image took about two minutes.

As we saw in the earlier experiment, the features on the sample changed. On top of that, the roughness of the film decreased as more images were taken. This is consistent with our theory. As we did earlier, we took $3\mu\text{m} \times 3\mu\text{m}$ images and $4\mu\text{m} \times 4\mu\text{m}$ images afterward to see the hole on the copper film. The following images are the results.

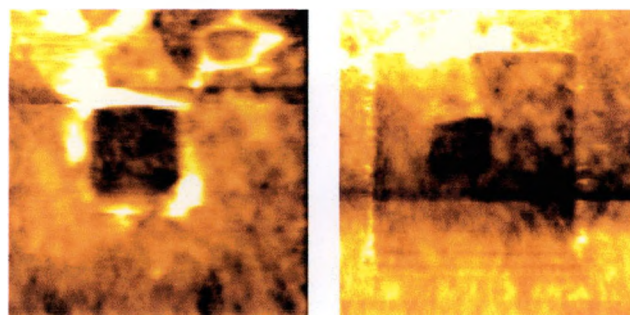


Figure 5.15 The image on the right is taken at $3\mu\text{m} \times 3\mu\text{m}$. We can see better square of $1\mu\text{m} \times 1\mu\text{m}$ in the image. The roughness is smaller than the images taken with the solution without BTA in it. The image on the right is $5\mu\text{m} \times 5\mu\text{m}$ image. Within the image, we are able to see both $1\mu\text{m} \times 1\mu\text{m}$ and $3\mu\text{m} \times 3\mu\text{m}$ squares.

One on the left is a $3\mu\text{m}\times 3\mu\text{m}$ image, and a square of about $1\mu\text{m}\times 1\mu\text{m}$ can be seen. The roughness inside of this square is 38.2\AA , and that of outside the square is 76.4\AA . This proves that CMP process used in the microelectronic fabrication industry can work at the atomic scale. The image on the right is a $4\mu\text{m}\times 4\mu\text{m}$ image. The interesting thing about this image is that not only we saw the $1\mu\text{m}\times 1\mu\text{m}$ square at the center, we can see where $3\mu\text{m}\times 3\mu\text{m}$ images are taken before this image was taken. The roughness inside the $1\mu\text{m}\times 1\mu\text{m}$ square is 35.8\AA , that of inside of square of $3\mu\text{m}\times 3\mu\text{m}$ without $1\mu\text{m}\times 1\mu\text{m}$ square is 111\AA , and that of inside of $4\mu\text{m}\times 4\mu\text{m}$ image without $3\mu\text{m}\times 3\mu\text{m}$ square is 143\AA . We can say that the area where the tip made contact with the sample is much smoother than elsewhere.

CHAPTER 6

VIDEO CAMERA FOR SPOTTING LASER ON CANTILEVER

6.1 Set Up

To spot laser on the cantilever, a regular microscope is used. A problem with this system was that every time we try to spot the laser, we had to peak through the microscope. To make spotting the laser on top of the cantilever easier we designed a video camera system. The system is shown in figure below.

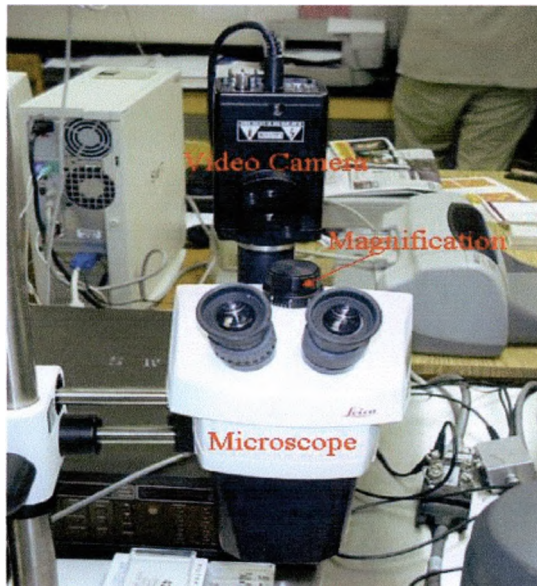


Figure 6.1 Video camera system designed to make focusing the laser beam on the top of the cantilever easier (the whole system can be seen in Figure 2.1).

Basic components of our video camera system are a microscope, a video camera that can be mounted on the microscope, a monitor, and a stand to hold both microscope and video camera.

6.1.1 Stand

The stand is capable of moving towards and away from the AFM using the ball bearing so that after spotting the laser on the cantilever, the microscope and the video camera slide so that we can cover the AFM with a lid for noise protection. The stand also can move in a circular motion for the same purpose.

6.1.2 Microscope

The microscope we use in this system is Leica GZ7 model, and it is focused using two knobs located front of it. These two knobs move the microscope vertically. A knob on the top of a microscope magnifies by up to seven times. A useful thing about this microscope is that we are able to peak through the microscope with eyes, without using the video camera and monitor.

6.1.3 Video Camera and Monitor

The video camera from Panasonic is easily mounted onto the microscope, which transfers the images to the monitor. If the images are not as bright as we want, we use a fiber optic illuminator to spot the cantilever for better images.

6.2 Resolution

To measure the resolution of video camera system we built, we first looked at one of two cantilevers we have in our lab, Microlever. The smallest feature on the Microlever is the width of the cantilever, indicated on the diagram below. The width of the smallest cantilever is $18\mu\text{m}$ so we knew then that the resolution of this system is smaller than $18\mu\text{m}$. Next we examined a $9.9\mu\text{m}$ grating used to calibrate AFM. When we measured a distance between thick lines, it was about 1mm . Because there are about 100 thinner

lines in between, we determined that each little grid we see on the diagram below is $9.9\mu\text{m}$. So that the resolution of this video camera system is believed to be less than $9.9\mu\text{m}$.

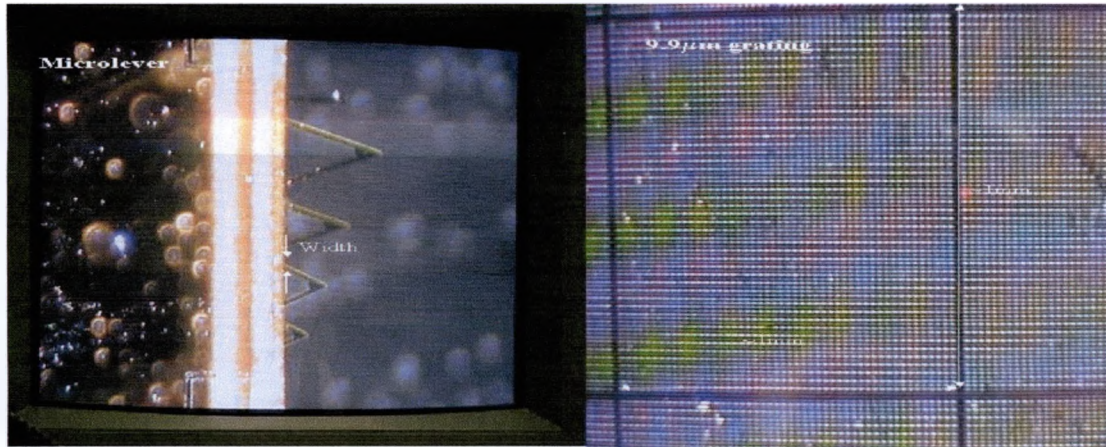


Figure 6.2 To see the resolution of the video camera system, we looked at two objects. One on the left is the Microlever, which has the smallest feature of $18\mu\text{m}$. We then looked at a $9.9\mu\text{m}$ grating, which we were able to see.

We believe that we do not need better resolution for our purpose right now. The only we do with this system is to focus the laser on top of the cantilever. As far as focusing on the cantilever, the resolution we have now is enough, as can be seen in the diagram.

CHAPTER 7

CONCLUSIONS

7.1 Scanning Capacitance Microscopy

In this thesis, we explained how Scanning Capacitance Microscopy (SCM) works, and how AFM must be modified to take capacitance images. We used SCM to measure the characteristics of the sample that was grown by Motorola. We performed four different experiments to see if our data were consistent with the data given by Motorola. The first experiment was to measure the capacitance of the sample as a function of voltage. As we expected, as we increased the voltage, the capacitance increased. We also fitted the curve to see that the second power function was more fitted than any other power function. The second experiment was to measure the capacitance as a function of set point. As we increased the set point, the capacitance decreased. This makes sense because if the tip is pressed firmly against the sample, the tip is not able to vibrate as much. The third experiment was the capacitance as a function of frequency. We began taking images at the resonant frequency. We both decreased and increased the frequency and took images to compare the images. As we expected, the signal was the highest when the image was taken at the resonant frequency. The last experiment we performed was to compare the capacitance at different positions of the wafer. We were told that the dielectric constant was about 40% higher in the center with respect to an edge point. We cut the wafer into four pieces and took capacitance images to verify. Our result was not consistent with their data.

7.2 Liquid Cell

We first explained the components needed to take AFM images in the liquid and how this technique is performed. We then showed the modifications we made to make imaging easier. Our main project for this thesis was to simulate Chemical Mechanical Polishing (CMP) process at the atomic scale using AFM. We first used nitric acid (HNO_3) without Benzotriazole (BTA) in the solution and a silica tip to see the reaction. The solution with BTA will create a monolayer of BTA molecules on top of the sample. As we see the results, we conclude that we created a hole where the tip made contact with the sample. We then used the same solution, but with BTA this time. As the result, we created better square hole on the sample where the tip made contact with the sample. We also decreased the RMS roughness of the sample, indicating that polishing as well as enhanced removal is occurring.

7.3 Future Work

With liquid cell, there are many experiments that we need to perform to understand how CMP process occurs. One improvement that we need to perform is to use a tub made out of Kel-F or other materials with low thermal expansion coefficient. By doing so, we will be able to decrease the thermal drift. We also need to use different type of the sample, the tip, the corrosion inhibitor, and the solution to understand the removal of different materials. To understand the characteristics of the different materials, we like to vary the set point to see if the removal rate relates to the set point. We would also like to vary the pH of the solution while images are taken to see if the removal rate varies with the pH of the solution. We will use the variable speed pump to perform this experiment.

To study the adhesive force between two materials, we can plot the force vs. distance curve. The following diagram shows how this technique works.

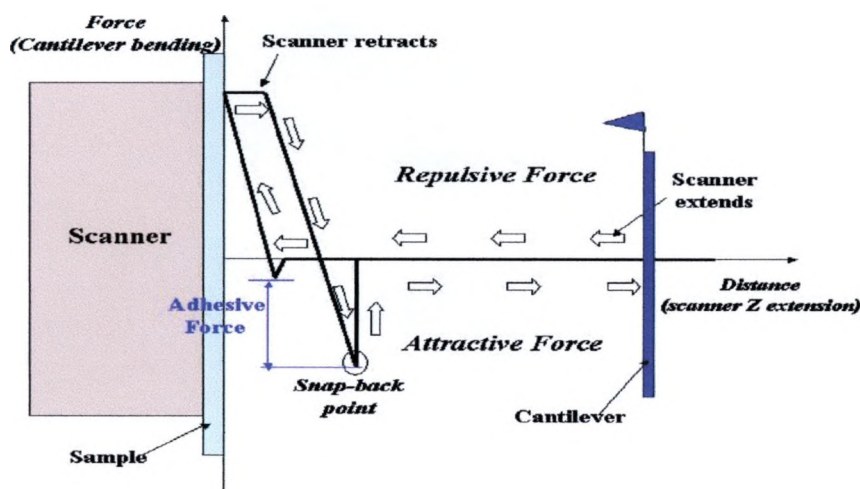


Figure 7.1 The force vs. distance curve

To plot this curve, the cantilever is lowered toward the sample. At some distance the cantilever does not feel any force, but at some point the cantilever is attracted toward the sample due to forces such as van der Waals force and then capillary force. Van der Waals is the electrostatic attractive force, and capillary force is the force due to layers of liquid on the surface. These attractive forces are then overcome by the repulsive force due to the electron clouds on the tip and atoms of the sample overlapping. When the tip and sample are not able to get closer, the cantilever bends. Due to few forces acting between the tip and sample, they are attached to each other for awhile. The cantilever feels the repulsive force first and then the attractive force before the cantilever actually snaps off the sample. This process can be seen in the diagram below. The adhesive force is the difference in forces at the point where the tip snaps onto the sample and the snap-back point indicated in the diagram.

BIBLIOGRAPHY

¹Dror Sarid, *Scanning Force Microscopy with Applications to Electric, Magnetic and Atomic Forces* (Oxford University Press, New York, 1994).

²Roland Wiesendanger, *Scanning Probe Microscopy and Spectroscopy* (Cambridge University Press, New York, 1994).

³Rebecca Howland and Lisa Benatar, "A Practical Guide to Scanning Probe Microscopy," , 1-73 (1996).

⁴Steffen Porthun, "High resolution magnetic force microscopy: Instrumentation and application for recording media," , University of Twente, 1996.

⁵C. F. Quate, "The AFM as a tool for surface imaging," *Surface Science* **299/300**, 980-995 (1993).

⁶Gabi Neubauer, Sidney R. Cohen, Gary M. McClelland *et al.*, "Force microscopy with a bidirectional capacitance sensor," *Review of Scientific Instruments* **61** (9), 2296-2308 (1990).

⁷S. Hudlet, M. Saint Jean, B. Roulet *et al.*, "Electrostatic forces between metallic tip and semiconductor surfaces," *Journals of Applied Physics* **77** (7), 3308-3314 (1994).

⁸R.C. Palmer, E. J. Denlinger, and H. Kawamoto, "Capacitive-Pickup Circuitry for VideoDiscs," *RCA Review* **42**, 95-112 (1978).

⁹J. K. Clemens, "Capacitive Pickup and the Buried Subcarrier Encoding system for the RCA VideoDisc," *RCA Review* (March 1978), 33-59 (1978).

¹⁰J. R. Matey, "Scanning capacitance microscopy," *Journal of Applied Physics* **57** (5), 1437-1444 (1984).

¹¹Hal Edwards, Rudy McGlothlin, Richard San Martin *et al.*, "Scanning capacitance spectroscopy: An analytical technique for pn-junction delineation in Si devices," *Applied Physics Letters* **72** (6), 698-700 (1997).

¹²V. V. Zavyalov, J. S. McMurray, and C. C. Williams, "Scanning capacitance Microscope methodology for quantitative analysis of p-n junctions," *Journal of Applied Physics* **85** (11), 7774-7783 (1998).

¹³M. L. O'Malley, G. L. Timp, S. V. Moccio *et al.*, "Quantification of scanning capacitance microscopy imaging of the pn junction through electrical simulation," *Applied Physics Letters* **74** (2), 272-274 (1998).

¹⁴A. Czerwinski, E. Simoen, and C. Claeys, "p-n junction peripheral current analysis using gated diode measurements," *Applied Physics Letters* **72** (26), 3503-3505 (1998).

¹⁵David J. Stein, Joseph L. Cecchi, and Dale L. Hetherington, "Atomic force microscopy, lateral force microscopy, and transmission electron microscopy investigations and adhesion removal mechanisms," *Journal of Materials Research* **14** (9), 3695-3706 (1999).

VITA

Yuji Yamaguchi was born in Osaka, Japan on March 16, 1976, the son of Keiko Yamaguchi and Nobumasa Oshitate. He decided to study in United States in 1990 and began attending San Marcos Baptist Academy in San Marcos, Texas. After graduating in 1993, he moved to Houston, Texas to attend Houston Community College. But in 1996, he realized that the education at Houston Community College was not taking him anywhere so he moved back to San Marcos, Texas to attend Southwest Texas State University. He received the degree of Bachelor of Science in physics in 1999. While he was attending Southwest Texas State University as an undergraduate student, he received Dean's List (1997-1999), Outstanding Beginning Physics Major (1998), Presidential Upper Level Scholarship (1998), and Outstanding Graduating Physics Major (1999). In August 2000, he decided to enter the Graduate School of Southwest Texas State University.

Permanent address: 2-102, 7-6 Kamisoshigaya
Setagaya-ku, Tokyo 157-0065
Japan

This thesis was typed by Yuji Yamaguchi

